Accepted Manuscript

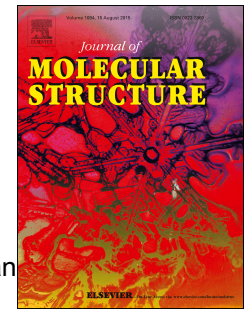

Spectroscopic, quantum mechanical and molecular docking studies of a new benzoxazole compound with an oxidoreductase enzyme and DNA

Celal Tuğrul Zeyrek, Bahadir Boyacioglu, Özlem Temiz-Arpaci, Hüseyin Ünver, Ayhan Elmali

PII: S0022-2860(17)30140-0

DOI: 10.1016/j.molstruc.2017.02.008

Reference: MOLSTR 23402

To appear in: *Journal of Molecular Structure*

Received Date: 10 October 2016

Revised Date: 30 January 2017

Accepted Date: 1 February 2017

Please cite this article as: C.T. Zeyrek, B. Boyacioglu, E. Temiz-Arpaci, H. Ünver, A. Elmali, Spectroscopic, quantum mechanical and molecular docking studies of a new benzoxazole compound with an oxidoreductase enzyme and DNA, *Journal of Molecular Structure* (2017), doi: 10.1016/j.molstruc.2017.02.008.

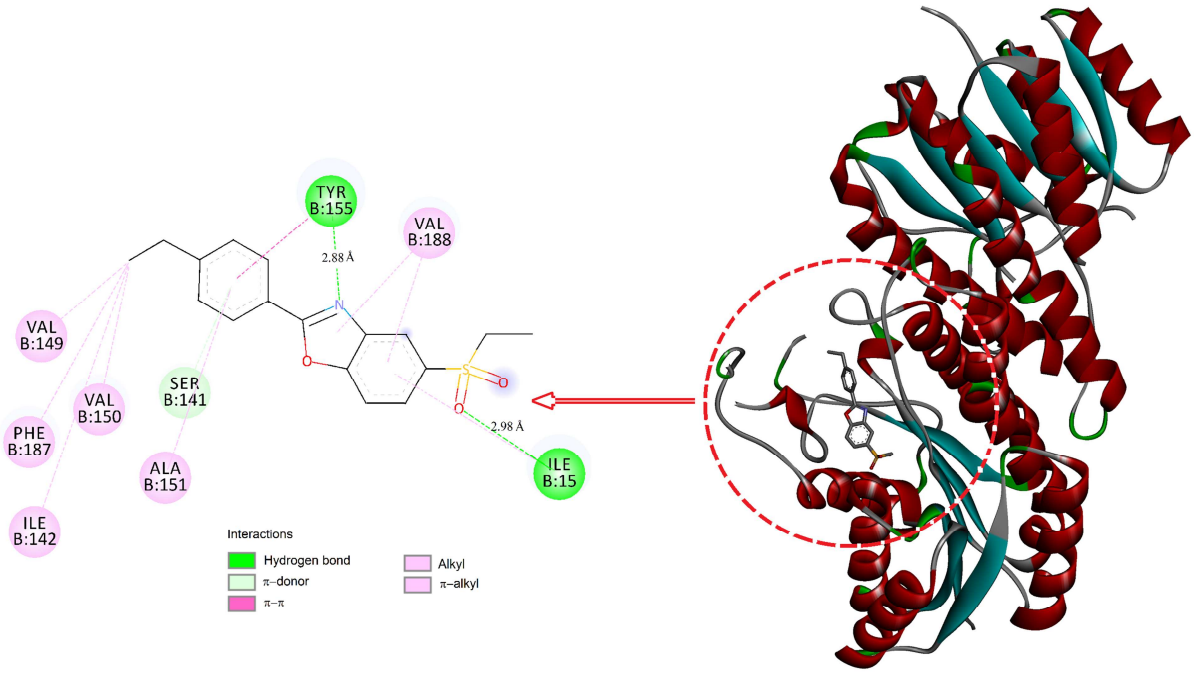

Spectroscopic, quantum mechanical and molecular docking studies of a new benzoxazole compound with an oxidoreductase enzyme and DNA

Celal Tuğrul Zeyrek[a,*], Bahadir Boyacioglu[b], Özlem Temiz-Arpaci[c], Hüseyin Ünver[d,*], Ayhan Elmali[e]

[a]Department of Training and Application, Ankara Nuclear Research and Training Center, Turkish Atomic Energy Authority, TR-06100 Beşevler, Turkey.

[b]Vocational School of Health Services, Ankara University, TR-06290 Kecioren-Ankara, Turkey.

[c]Department of Pharmaceutical Chemistry, Faculty of Pharmacy, Ankara University, TR-06100, Beşevler, Turkey.

[d]Department of Physics, Faculty of Sciences, Ankara University, TR-06100, Beşevler , Turkey.

[e]Department of Physics Engineering, Faculty of Engineering, Ankara University, TR-06100, Beşevler , Turkey

∗Corresponding authors. *Tel.:* +90-312-2126230; *fax:* +90-312-2226421 (C.T.Zeyrek)

Tel: +90- 312 2126720-1108 (H. Ünver)

E-mail address: zeyrek@taek.gov.tr, ctzeyrek@gmail.com (C. T. Zeyrek)

unverh@ankara.edu.tr (H. Ünver)

Abstract

The spectroscopic, theoretical molecular structure, full vibrational band assignments, MEP, NBO, frontier molecular orbitals, and NLO effects, and molecular docking studies of 5-ethylsulphonyl-2-(p-ethylphenyl)-benzoxazole, $C_{17}H_{17}SO_3N$, (**L**) have been presented in this work. The quantum mechanical calculations have been performed by using the Hartree-Fock (HF)/6-311++G(d,p) and density functional theory (DFT) with the B3LYP/6-311++G(d,p) levels. Calculated vibrational frequencies have been compared with the experimental FT-IR spectra. The natural bond orbital (NBO) analysis has been performed to determine the hyper conjugative interactions. Frontier molecular orbitals have been defined to predict the chemical parameters of the **L**. The first order hyperpolarizability of **L** was calculated to find its role in nonlinear optics. Molecular docking of **L** with the oxidoreductase enzyme nicotinamide adenine dinucleotide phosphate (NADPH) exhibited the good binding affinity with energy of −8.8 kcal/mol. The molecular docking was also done to identify the interaction of **L** with the DNA.

Keywords: Benzoxazoles; spectroscopy; molecular docking; DFT; oxidoreductase, DNA

1. Introduction

The benzoxazole derivatives are compounds that have significant technological use in bioorganic medicinal and optical fields. First of all, considering the application benzoxazoles in the bioorganic medicinal applications, the benzoxazoles show an important role biological activities such as antibiotic [1], antimicrobial [2-4], antiviral [5], topoisomerase I and II inhibitor [6], multidrug resistance cancer cell activities [7] and antioxidant activities [8]. Fighting against bacterial infections has resulted in the development of a wide variety of antibiotics. There is still need for new antifungal and antibacterial agents. Therefore, they have been under investigation because of their potential applicability biological agents in the pharmaceutical chemistry.

An oxidoreductase is an enzyme that catalyzes the transfer of electrons from one molecule, the reductant, also called the electron donor, to another, the oxidant, also called the electron acceptor. This group of enzymes usually utilizes nicotinamide adenine dinucleotide phosphate (NADP, NADP+ or NADPH) as cofactors [9]. The major source of NADPH in animals and other non-photosynthetic organisms is the pentose phosphate pathway. However, there are several other lesser-known mechanisms of generating NADPH, all of which depend on the presence of mitochondria. The first and rate-limiting step of steroidogenesis is catalyzed by the mitochondrial cholesterol side chain cleavage system that is dependent on NADPH [10]. NADPH is used for anabolic pathways, such as lipid synthesis, cholesterol synthesis, and fatty acid chain elongation. The NADPH system is also responsible for generating free radicals in immune cells. These radicals are used to destroy pathogens in a process termed the respiratory burst. It is the source of reducing equivalents for cytochrome P450 hydroxylation of aromatic compounds, steroids, alcohols, and drugs. NADPH also provides the reducing equivalents for biosynthetic reactions and the oxidation-reduction involved in protecting against the toxicity of ROS (reactive oxygen species), allowing the regeneration of GSH (reduced glutathione) [11]. According to the Prediction of Activity Spectra (PASS) analysis results [12], to evaluate the inhibitory nature of 5-ethylsulphonyl-2-(p-ethylphenyl)-benzoxazole against NADPH enzyme, molecular docking

studies were performed. Also the anticancer activities of the benzoxazole derivatives and their binding studies with DNA have been intensively investigated since they show important anticancer activity and significant DNA-binding ability [8, 13, 14]. To understand the drug-DNA interaction molecular docking is also used. Structurally different molecule binds with DNA in different fashion, respectively. Molecular docking study was performed to understand the interaction mechanism between the investigated compound and DNA, and the preferred molecular orientation in B-DNA.

The large second order electric susceptibility of organic materials is very important because of its potential usability as organic molecular devices such as nonlinear optical (NLO) devices, frequency converters, electro optical modulators. The second order electric susceptibility is related to the first hyperpolarizabilty the search for organic chromophores with large first hyperpolarizabilty are fully justified. For this reason, the benzoxazoles derivatives also attracted a wide attention to the researcher for their diverse range of optical activities. Its derivative is one of the most promising groups of light-emitting devices (LED) [15-17].

So that in the present study, we aimed to synthesize 5-ethylsulphonyl-2-(p-ethylphenyl)-benzoxazole (**L**), to compared experimental and theoretical results, to reveal the optimized molecular structural parameters, vibrational spectra, NBO, MEP, HOMO-LUMO analyses, nonlinear optical (NLO) effects for **L**. The molecular docking study is also reported to reveal the interaction of **L** with the NADPH and DNA.

2. Materials and methods

2.1. The synthesis and techniques

The chemicals were supplied from the commercial venders. The 5-Ethylsulphonyl-2-(p-ethylphenl)-benzoxazole (**L**) was synthesized by using the methods in the literature [2, 15]. The diagram of the synthesis is given in Scheme 1. Formula; $C_{17}H_{17}SO_3N$, M.p.;142 °C, Yield; 35 %. MS(ESI+) m/z (%X): 316(%16)(M+1). The melting point of the **L** was taken on a Buchi SMP 20

capillary apparatus. IR spectra were recorded on a Jasco FT/IR-420 spectrometer as KBr discs. ^{1}H NMR and ^{13}C NMR (with HSQC) spectra were obtained with a Varian 400 MHz spectrometer in $CDCl_3$ and tetramethylsilane (TMS) was used as an internal standard. Mass analysis was carried out with a Waters Micromass ZQ by using ESI (+) method.

2.2.Calculation details

2.2.1. HF and DFT calculation

The molecular geometry of **L** is created and fully optimized by used at in the Gaussian 09 and the Gauss-view program [18, 19]. Geometry optimization of the **L** was performed by using HF/6-311++G(d,p) and DFT/B3LYP (Becke's three parameters hybrid exchange-correlation functional)/6-311++G(d,p) level [20-22]. The vibrational frequencies were determined by using the optimized structure. The vibrational wavenumbers for the **L** were calibrated by using quantum mechanics force field (SQMFF) methodology [23]. The potential energy distributions (PED) of each vibrational mode were calculated by using SQM program [24]. ^{1}H and ^{13}C NMR chemical shifts were calculated using a gauge invariant atomic orbital (GIAO) approach [25]. Molecular electrostatic potential (MEP) surface was confirmed by using the same level of theory. The total energies, frontier molecular orbitals energies and band gaps were calculated by the B3LYP/6-311++G(d,p) level. The chemical hardness (η) were calculated according to the Koopmans theorem [26]. The NBO analysis of the investigated compound was carried out at the same level by using the NBO 3.1 program [27]. The NLO parameters such as the total molecular dipole moment (μ_{tot}), linear polarizability (α_{ij}), and the first-order hyperpolarizability (β_{ijk}) of **L** were determined by the B3LYP/6-311++G(d,p) level.

2.2.2. Molecular docking calculations

In our present work, we have tried to dock title compound (**L**) to one of the target oxidoreductase enzyme nicotinamide adenine dinucleotide phosphate (NADPH) (PDB ID: 5B1Y) and to B-DNA protein (PDB ID: 1BNA). Prediction of Activity Spectra (PASS) [12] analysis (PASS) of **L** is given in Table S1 (supplementary material). This analysis predicts oxidoreductase

inhibitor activity with P_a (probability to be active) value of 0.407. According to the PASS analysis, to evaluate the inhibitory nature of the title compound against NADPH enzyme and to understand the interaction mechanism between the investigated compound and B-DNA, and the preferred molecular orientation in B-DNA, molecular docking studies were performed. High resolution 3D crystal structures of NADPH enzyme (PDB ID: 5B1Y) [9] and B-DNA protein (PDB ID: 1BNA) [28] were downloaded from the protein data bank.

The AutoDock-Vina software [29] and AutoDockTools (ADT) were used for molecular docking calcuations. The polar hydrogens and Kollman atomic charges were added to the target NADPH enzyme by used ADT graphical. Water molecules were removed and the partial charges were added by Geistener method before the docking calculations. The active site of the enzyme was defined to include residues of active site within the grid size of 40x40x40 Å for NADPH enzyme and 20x20x30Å for B-DNA protein. Receptor-ligand interactions were illustrated with PyMol and Discover Studio Visualizer 4.0 software [30, 31].

3. Results and discussions

3.1.Optimized geometry

The calculated structural parameters of **L** and the experimental values of the similar benzoxazoles compounds in the literature are given in Table 1. There is not X-ray crystallographic data of **L**, but the calculated structural parameters are almost comparable with the reported structural parameters of the similar benzoxazoles compounds. The **L** consists of the para-substituted phenyl ring PhI [C10-C15], ethyl group [C16, C17], trisubstitued phenyl ring PhII, benzoxazole RingIII [C3-C9, N1, O1] and the ethylsulphonyl group [S1, O2, O3, C1, C2]. The optimized geometry shows in Figure 1.

As an optimized geometry, whole of moieties is nearly planar. The torsion angles for ethylsulphonyl moiety with the PhII are C5–C4–C3–S1= -179.19 (HF), 179.80^o (B3LYP), C1–C2–S1–C3= -66.63 (HF), -67.44^o (B3LYP), and C2–S1–C3–C4= -96.25 (HF)^o, -96.02^o (B3LYP).

The ethyl group is titled from the para-substituted phenyl ring PhI which is evident from the torsion angles C12-C13-C16-C17=87.44 (HF), 89.11^{o} (B3LYP), and C14-C13-C16-C17=-91.27 (HF), 89.21^{o} (B3LYP), accordingly. The oxygen atoms bonded with S1 atom of the ethylsulphonyl group are in a non-tetrahedral configuration with the angle O3–S1–O2 of 120.09 (HF), 120.99^{o} (B3LYP). The distorted tetrahedral arrangements were generally also observed in the sulphonamid derivatives in the literature [15, 32-35]. The calculated bond angles of C2–S1–C3 are 106.34 (HF), 105.46^{o} (B3LYP). They are smaller than the tetrahedral angle value (109^{o}). The N1–C9 distance of 1.271 (HF), 1.297 (B3LYP) Å is normal double N=C bond value, respectively [15, 36, 37]. The range of C-C bond distances of the aromatic rings are 1.380–1.391 (HF), 1.388–1.403 Å (DFT) in PhI, 1.382–1.398 (HF), 1.393–1.405 Å (DFT) in PhII. The optimized bond lengths using the DFT are commonly longer and more accurate than HF due to the inclusion of electron correlation [15, 38-41]. According to these results, it may be concluded that the B3LYP/6-311++G(d,p) level calculations well reproduce the bond distances and the bond angles. The calculated structural parameters are good agreement with the experimental values of the similar compound in literature [15, 35, 37, 41-47] (Table 1).

3.2. ^{1}H and ^{13}C NMR spectroscopy

The GIAO ^{1}H and ^{13}C NMR chemical shift values (with respect to TMS) were calculated by the B3LYP/6-311++G(d,p) level and compared to the experimental ^{1}H and ^{13}C NMR chemical shift values (Figure 2) in Table 2. The two-dimensional (2D) heteronuclear chemical shift correlation (HSQC) was given in Figure 2c.

^{1}H NMR spectrum of the **L**, the aromatic protons appeared as a broad band at 7.39-8.31 ppm, while the computational results are predicted at 7.61-8.71 ppm for $CDCl_3$, 7.45-8.73 ppm for gas phase. The protons in phenol groups give rise to a signal in the interval 4-7.5 ppm, depending on concentration, solvent and temperature [48]. But the phenolic proton under intra-intermolecular hydrogen bonding interaction gives a resonance signal between 10–12 ppm [48].

In the ^{1}H NMR spectrum, 1.32 and 1.30 ppm triplets specify the protons of two methyl group. The quartet peaks at 3.17 and 3.68 ppm specify the two ethyl group protons in the ^{1}H NMR spectrum. The ethyl group protons of ethylsulphonyl moiety are assigned to the chemical shift 2.96 and 3.07 ppm in solvent phase, while the ethyl group protons of para- substituted phenyl ring PhI moiety are assigned to 2.69 and 2.70 ppm in solvent phase. The methyl group protons of the para- substituted phenyl ring PhI moiety are calculated in the range of 1.42, 1.06, 0.69 ppm for $CDCl_3$ and 1.51, 0.87, 0.60 ppm in gas phase. These bands are calculated at 1.42, 1.08, 1.07 ppm in $CDCl_3$ and 1.38, 1.09, 1.07 ppm in gas phase for para- substituted phenyl ring PhI moiety.

The large electron density over the nuclei leads to low chemical shift values due to shielding effect and less electron density over the nuclei gives high ppm values because of deshielding effect. Aromatic carbons give signals in overlapped areas of the spectrum with chemical shift values from 100 to 200 ppm [49, 50]. The observed experimental chemical shift positions of ring carbons of the title compound lie in the range 123.57– 149.50 ppm. The cumulative high electronegativity of nitrogen and oxygen in the benzoxazole RingIII ring reduces the electron density of the carbon atom C9, thus its NMR signal is observed in the very downfield at 165.65 ppm. This peak calculated at 171.18 ppm in gas phase and 172.16 ppm in $CDCl_3$. The carbon atoms C5 and C6 are also in the downfield due to the deshielding effect of the electronegative atoms N1 and O1. The oxygen atom is more electronegative than nitrogen and hence the chemical shift of C6 (153.73 ppm) is relatively in the more downfield than C5 (142.84 ppm). These peaks theoretically appeared at 159.21 ppm in gas phase, 159.86 ppm in $CDCl_3$ and 148.66 ppm in gas phase, 148.48 ppm in $CDCl_3$, respectively. The sulfur atom is less electronegative than oxygen and nitrogen hence the chemical shift of C3 (135.10 ppm for experimentally, 146.26 ppm for gas pahse and 145.43 for $CDCl_3$ for DFT) is relatively in the less downfield than C6 and C5. The corresponding theoretical chemical shift values are found in good agreement with calculated chemical shift values (Table 2).

3.3.Vibrational band assignments

The compound **L** have 111 vibrational normal modes because of it consists of N=39 atoms and gives 3N-6 modes. The observed FT-IR bands and calculated wavenumbers with vibrational band assignments which were performed at B3LYP/6-311++G(d,p) theory level are given in Table 3. The theoretical and experimental IR spectrums are shown in Figure 3.

The CH stretching vibrations in aromatic group are expected between 3120 and 3000 cm^{-1} [51]. These vibrations bands are calculated in the range 3106-3056 cm^{-1} for PhI and 3076-3059 for PhII by using the B3LYP/6-311++G(d,p) level. Experimentally, we has observed band at 3052 cm^{-1} for the aromatic CH stretching vibrations.

The symmetric and asymmetric stretching vibrations of CH_2 and CH_3 are anticipated in the range 2900-2950 and 2950-3050 cm^{-1} [51, 52]. The bands at 2969 and 2925 cm^{-1} are assigned to the symmetric stretching CH_2 and CH_3 modes. These bands were calculated at 2958 and 2915 (pure symmetric stretching vibrations of CH_2 with 97% contribution of PED) and 2909 cm^{-1} (pure symmetric stretching vibrations of CH_3 with 96% contribution of PED).

In many molecules, the asymmetrical deformations of CH_3 are observed in the range 1495–1435 cm^{-1} [52], while the symmetric deformations CH_3 are expected in the range 1380 ± 25 cm^{-1} [53]. The asymmetrical deformation of CH_3 was observed at 1455 cm^{-1}. The calculated values of asymmetrical deformations CH_3 modes are at 1483 and 1472 cm^{-1} with 52% and 53% pure contribution of PED, while the symmetrical deformation of CH_3 was calculated at 1405 and 1401 cm^{-1} with 40% and 52% pure contribution of PED.

The scissoring vibrations of CH_2 are expected in the regions 1455±55 and 1350±85 cm^{-1} [53, 54]. The scissoring CH_2 modes were assigned at 1472 and 1438 cm^{-1} for B3LYP/6-311++G(d,p) level.

The C=N stretching bands are expected in the range 1670–1500 cm^{-1} [48, 53], while the C–N stretching vibration is reported in the range 1000-1200 cm^{-1} [53]. In the present study, C=N stretching mode is assigned at 1553 cm^{-1} in the IR spectrum and at 1550 cm^{-1} with 22% mixed

contribution of PED theoretically. Zeyrek *et. al* [15] reported C–N stretching vibration theoretical value 1581 cm^{-1} for 2-(4-bromobenzyl)-5-ethylsulphonyl-1,3-benzoxazole, Parveen *et al.* at 1526 cm^{-1} [55] for 5-ethylsulphonyl-2-(p-aminophenyl)benzoxazole, and Mary *et. al* [56] at 1536 cm^{-1} for 2-(p-fluorobenzyl)-6-nitrobenzoxazole theoretically. For the title compound, the C–N stretching mode was assigned at 1230 cm^{-1} for B3LYP level.

The S=O asymmetric and symmetric stretching vibrations are reported in the range 1330±60 and 1180±45 cm^{-1} [52]. The symmetric stretching mode was observed at 1042 cm^{-1}, while DFT calculations give these modes at 1077, 1034 and 1028 cm^{-1} with different % PED values. The asymmetric stretching mode was observed at 1243 cm^{-1}. The asymmetric stretching modes were calculated at 1248 and 1226 cm^{-1} with 10% and 73% mixed contribution of PED. The deformation modes of SO_2 are assigned at 523 cm^{-1} for FTIR and 504 cm^{-1} for theoretically with 17% PED value. This modes are reported at 577, 451, 379, 308 cm^{-1} [55] and 575, 457, 390 and 298 cm^{-1} [56] theoretically for similar benzoxazole derivatives. C–S stretching bands are assigned at 717, 668 and 609 cm^{-1} as expected [57] and reported values are 655 and 699 cm^{-1} [55], 704 and 663 cm^{-1} [56] for a similar compounds.

The stretching modes of the phenyl rings are expected in the range 1620–1280 cm^{-1} [51]. These vibrations are observed at 1620 and 1306 cm^{-1} for PhI, 1620, 1596, 1553, 1415, 1279 cm^{-1} for PhII. The stretching vibrations of the PhI and PhII are assigned at 1617, 1610, 1600, 1570, 1550, 1503, 1454, 1425, 1419, 1347, 1328, 1277, 1259 and 1247 cm^{-1} by the DFT calculations. In the present study, ring breathing mode is observed at 784 cm^{-1} in FTIR and calculated at 776 cm^{-1} for PhI. The comparison data of the experimental and calculated vibrational band assignments are given in Table 3.

3.4.NBO analysis

To provide information about the interaction in filled and virtual orbital spaces and to analysis about intra- and intermolecular interactions among bonds the NBO analysis is useful method. For that purpose the stabilization energies of **L** were computed by using second-order

perturbation theory at B3LYP/6-311++G(d,p) level. The selected stabilization energies (larger than 3 kcal/mol), the natural bond orbital occupancies, energy difference between donors and acceptors and Fock matrix elements of the investigated compound are given in Table 4. The atoms in the ring PhI and ring PhII with benzoxazole RingIII have ordinary single-double configuration that form the conjugate structure. The NBO occupancy values of single S1–O2 and S1–O3 are1.98328 and 1.98283, respectively. It is indicated that they have same level in the ethylsulphonyl group. The NBO analysis is also indicated that the N1–C9 in the RingIII has the double bond character. The NBO analysis confirms the optimized theoretical molecular geometry of the investigated compound.

The intramolecular hyperconjugative interaction of the σ(N1–C5) distribute to σ*(N1–C9) stabilization of 5.96 kcal mol^{-1} in the RingIII. This enhanced further conjugate with antibonding orbital π*(C6–C5) which results to strong delocalization of 15.99 kcal mol^{-1}. The lone pair of O1 donates its electrons to the π-type anti bonding orbital for (N1–C9). This interaction gives the strongest stabilization to the system of the compound by 37.94 kcal mol^{-1}.

3.5. MEP surface

MEP is an extremely valuable tool for the description for the non-covalent interactions, especially hydrogen bonds. To investigate reactive sites in the compound, the MEP surface was predicted by DFT calculation at the B3LYP/6-311++G(d,p) level. As a result of the MEP surface, negative regions (electrophilic reactivity) and positive regions (nucleophilic reactivity) shown in Figure S1 (supplementary material). So, there are two possible regions for electrophilic reactivity in the compound. The oxygen atoms O2 and O3 of the ethylsulphonyl group are in the negative sites. The maximum values of 0.059 a.u. for O2 and 0.058 a.u. for O3 in the negative sites are pointing out possible sites for electrophilic reactivity, while a value of 0.021 a.u. the region on the C7-H7 bond is emphasizing a possible site for nucleophilic reactivity in the whole molecule. These regions give preliminary information about to predict intermolecular interactions.

3.6.Chemical reactivity descriptors

The frontier molecular orbitals (HOMOs and LUMOs) are the very important parameters for chemical reactivity because of these orbitals are directly related to the ionization potential and the electron affinity, respectively. The HOMO and LUMO energies of the **L** were predicted by the B3LYP/6-311++G(d,p) level. By using the HOMO and LUMO energy values for **L**, HOMO-LUMO band gap and the global chemical reactivity descriptors of molecules such as chemical hardness (η), electronegativity (χ), softness (σ), chemical potential (μ_p), and electrophilicity index (ω) as well as local reactivity have been defined according to the Koopmans theorem [26]. The calculated chemical parameters of the title compound are η=2.2587, χ=4.3828, σ=0.4424, μ_p=-4.3828 eV and ω=9.6045. These values were listed in Table 5. The chemical hardness is proportional the relative stability and reactivity of chemical compounds. The large HOMO-LUMO band gap (4.5174 eV) means a hard molecule whereas small band gap means a soft molecule. The HOMO–LUMO energy gap value for **L** was calculated to be 4.5174 eV in gas phase. The HOMO–LUMO energy gap value is very important to application of the novel benzoxazole derivative for using a light-emitting element [15-17] in the technology.

The distributions and energy levels of the HOMO-1, HOMO, LUMO and LUMO+1 of **L** are shown in Figure 4. As seen in Figure 4, characteristics of these orbitals is π-type molecular orbital.

Except for ethylsulphonyl and ethyl moieties in the structure, the LUMO, HOMO and HOMO-1 are mostly localized on the complete molecule of **L**, while the LUMO+1 is localized are mainly localized on the trisubstitued phenyl ring PhII with benzoxazole RingIII except for CH_3 group in gas and solvent (dimethyl sulfoxide) phases (Figure 4).

3.7. Nonlinear Optical (NLO) Effects

NLO properties of the molecules are very considerable in supplying the main functions of optical devices such as optical modulation, optical switching and optical storage in the

telecommunications, signal processing and optical interconnections technologies [58]. To understand between the structure and NLO properties, theoretical approach can play an important role. For this purpose, the total molecular dipole moment (μ), linear polarizability (α), and the first-order hyperpolarizability (β) of **L** were predicted by the B3LYP/6-311++G(d,p) level. The predicted values of μ_{tot}, α_{tot} and β_{tot} and their *x*, *y*, *z* components are listed in Table S2 (supplementary material). The μ_{tot} was predicted to be 7.511 Debye and its highest component was found to be the one denoted by μ_x (2.1133 Debye), while the smallest component was μ_y (0.3942 Debye).

The value of hyperpolarizability (β_{tot}) is an indication for the NLO activity of the molecular system. The value of β_{tot} shows the intramolecular charge transfer resulting from the electron cloud movement through π-conjugated frame work from electron. The calculated value of β_{tot} for **L** is 6.9285×10^{-30} cm^5/esu which is 53.3 times that of the standard NLO material urea (0.13×10^{-30} cm^5/esu) [59]. The calculated values β_{tot} of **L** and similar benzoxazoles compounds [15, 60-62] in the literature are given in Table 6 for the comparison. The calculated values of β_{tot} in **L** are smaller than that 5-nitro-2-(4-nitrobenzyl) benzoxazole ($\beta_{tot} = 8.47 \times 10^{-30}$ cm^5/esu) calculated with B3LYP/6-3G* level [61], and greater than that of other similar compounds given in Table 6 [15, 60, 62].

3.8. Molecular docking studies of L with NADPH

Benzoxazole derivatives mainly present involved in research possess interesting biological activities like antifungal [3], antitumor, anti-cancer [7], anti-HIV [63]. An oxidoreductase is an enzyme that catalyzes the transfer of electrons from one molecule, the reductant, also called the electron donor, to another, the oxidant, also called the electron acceptor. This group of enzymes usually utilizes nicotinamide adenine dinucleotide phosphate (NADP, $NADP^+$ or NADPH) as cofactors [9].

The docking protocol was tested by removing co-crystallized inhibitor from the protein and then docking it at the same site (Figure 5a). The docking results were accepted as correct

when the RMSD value was lower than 2Å [64]. This value indicates the deviation of the ligand form the active site with which it interacts, and it is the most important criterion used for docking results. The criterion to be considered after RMSD is the bonding energy. The reason behind this priority order is that the structure may give low bonding energy outside the active site as well. The predicted bonding energy as a result of molecular docking and RMSD values are given comparatively in Table 7. Energetically most favorable docked structures obtained from the rigid molecular docking of the compound **L** with 5B1Y are shown in Figure 5b. The **L** binds at the active site of the NADPH by weak non-covalent interactions most prominent of which are H-bonding, π-donor, π-π, alkyl and π-alkyl interactions as shown in Figure 6. TYR15 and ILE15 amino acids form H-bond with nitrogen atom of the benzoxazole RingIII and oxygen atom of ethylsulphonyl group with distances of 2.88 and 2.98 Å. VAL188 and ILE15 form π-alkyl interaction with trisubstitued phenyl ring PhII and benzoxazole RingIII. PHE187 also forms π-alkyl interaction with methyl group of **L**. ILE142, VAL149, and VAL150 form alkyl interaction with methyl group of **L**. TYR155 form π-π interaction with phenyl ring PhI of **L**. Binding free energy (ΔG in kcal/mol) of -8.8 as predicted by Autodock Vina (Table 7) suggests good binding affinity between the ligand L and the target NADPH macromolecule. It is evident that both the nitrogen atom of benzoxazole RingIII and oxygen atom of ethylsulphonyl group are crucial for binding. These results draw us to the conclusion that the investigated compound might exhibit oxidoreductase inhibitor activity. However biological tests need to be done to validate the computational predictions.

3.9. Molecular docking studies of L with B-DNA

To understand the drug-DNA interaction molecular docking is used. Structurally different molecule binds with DNA in different fashion, respectively. Molecular docking study was performed to understand the interaction mechanism between the investigated compound B-DNA (PDB ID: 1BNA), and the preferred molecular orientation in B-DNA. The predicted bonding

energy as a result of molecular docking and RMSD values are given comparatively in Table 7. Energetically most favourable docked structures obtained from the rigid molecular docking of the compound with 1BNA (B-DNA) is shown in Figure 7 (a). The relative binding energy of docked the compound-(B-DNA) are found to be -8.0 kcal/mol. The compound binds at the active site of the 1BNA for B-DNA proteins by weak non-covalent interactions most prominent of which are conventional H-bond, π-anion, π-sulfur, and CH···O. These interactions are illustrated shown in Figure 7 (b). The resulting docked pose of **L**-(B-DNA) reveals that oxygen atom of ethylsulphonyl group binds on the surface of the DNA where O atom of ethylsulphonyl is involved in hydrogen bonding (3.01 Å) with nitrogen atom (N2) of guanosine (A:DG10:N2). Hydrophobic interaction and van der Waals interactions are also present in the complex (Figure 7 b). According to the calculated bonding affinities, these initial results show that the investigated compound might inhibit the DNA protein.

4. Conclusion

In the study, synthesis, theoretical molecular structure, FT-IR, ^{1}H and ^{13}C NMR investigations, vibrational band assigned, MEP, NBO analysis, frontier molecular orbitals, NLO effects, antimicrobial activity and molecular docking study of **L** have been presented. The theoretical 3D-geometric parameters values of **L** were quite agreement with the experimental values of the similar compound in literature. Complete vibrational assignments of the experimental and calculated FTIR bands have been proposed on the basis of PED analysis and most of the modes have wavenumbers in the expected range. According to the MEP surface of the compound, the oxygen atoms of ethylsulphonyl group have maximum negative region indicating an electrophilic attack, while C7-H7 bond region has a maximum positive region indicating a possible site for nucleophilic attack. The energy separation between the HOMO and LUMO is found to be 4.5174 eV. The value of hardness is predicted at 2.2587 eV. Common problems with OLEDs include fast aging/short life span, undesirably high operating voltages, or insufficient

efficiency. Thus, here is a need for new compounds for OLED devices that enable long-lasting and highly efficient devices. Compounds with these characteristics typically require specific HOMO and LUMO energy levels, and a sufficient energy gap between HOMO and LUMO. In this context, if the HOMO-LUMO gap of the investigated benzoxazole compound is compared with the HOMO-LUMO gaps of the similar benzoxazole derivatives used in the light emitting elements, the compound **L** may be a good candidate as a light emitting element. Also, the investigated compound is a good candidate as a nonlinear optical material since the calculated value of β_{tot} for the title compound is 53.3 times that of the standard NLO material urea.

The docking simulation process was used to obtain possible bonding models and confirmations for the title compound according to the PASS analysis. The investigated compound binds at the active sites of the NADPH and B-DNA by weak non-covalent interactions. Molecular docking studies showed that promising **L**, directly interacted with active site of the NADPH by weak non-covalent interactions most prominent of which are H-bonding, π-donor, π-π, alkyl and π-alkyl interactions. The resulting docked pose of L-(B-DNA) also reveals that oxygen atom of ethylsulphonyl group binds on the surface of the DNA where O atom of ethylsulphonyl is involved in hydrogen bonding (3.01 Å) with nitrogen atom (N2) of guanosine (A:DG10:N2). The molecular docking results draw us to predict the binding of drug candidates a receptor (NADPH and B-DNA) of known 3D structure and **L**.

As a result, in this study, new promising bioactive compound (**L**) was designed and synthesized by a simple and efficient method, followed by the evaluation of their biological activities. On the basis of experimental and computational results of **L**, it can be concluded that this work will be useful for the design and synthesis of new materials for further study in bioorganic medicinal and optical fields.

References

[1] M. Prudhomme, J. Guyot, G. Jeminet, Semisynthesis of A23187 (Calcimycin) Analogs .4. Cation Carrier Properties in Mitochondria of Analogs with Modified Benzoxazole Rings - Antimicrobial Activity, J Antibiot 39(7) (1986) 934-937.
[2] M. Arisoy, O. Temiz-Arpaci, F. Kaynak-Onurdag, S. Ozgen, Synthesis and Antimicrobial Activity of Novel Benzoxazoles, Z Naturforsch C 67(9-10) (2012) 466-472.
[3] M. Arisoy, O. Temiz-Arpaci, F. Kaynak-Onurdag, S. Ozgen, Novel Benzoxazoles: Synthesis and Antibacterial, Antifungal, and Antitubercular Activity against Antibiotic-Resistant and -Sensitive Microbes, Z Naturforsch C 68(11-12) (2013) 453-460.
[4] M. Arisoy, O. Temiz-Arpaci, F. Kaynak-Onurdag, S. Ozgen, Synthesis and Antimicrobial Evaluation of 2-(p-Substituted Phenyl)-5-[(4-substituted piperazin-1-yl)acetamido]-benzoxazoles, Z Naturforsch C 69(9-10) (2014) 368-374.
[5] D.N. Ward, D.C. Talley, M. Tavag, S. Menji, P. Schaughency, A. Baier, P.J. Smith, UK-1 and structural analogs are potent inhibitors of hepatitis C virus replication, Bioorg Med Chem Lett 24(2) (2014) 609-612.
[6] A. Pinar, P. Yurdakul, I. Yildiz, O. Temiz-Arpaci, N.L. Acan, E. Aki-Sener, I. Yalcin, Some fused heterocyclic compounds as eukaryotic topoisomerase II inhibitors, Biochem Bioph Res Co 317(2) (2004) 670-674.
[7] H. Lage, E. Aki-Sener, I. Yalcin, High antineoplastic activity of new heterocyclic compounds in cancer cells with resistance against classical DNA topoisomerase II-targeting drugs, Int J Cancer 119(1) (2006) 213-220.
[8] O. Temiz-Arpaci, T. Coban, B. Tekiner-Gulbas, B. Can-Eke, I. Yildiz, E. Aki-Sener, I. Yalcin, M. Iscan, A study on the antioxidant activities of some new benzazole derivatives, Acta Biol Hung 57(2) (2006) 201-209.
[9] Y. Fukuda, T. Araki, T. Ohshima, K. Yoneda, Catalytic properties and crystal structure of thermostable NAD(P)H-dependent carbonyl reductase from the hyperthermophilic archaeon Aeropyrum pernix K1, Enzyme and Microbial Technology 91 (2016) 17-25.
[10] I. Hanukoglu, R. Rapoport, Routes and Regulation of Nadph Production in Steroidogenic Mitochondria, Endocrine Research 21(1-2) (1995) 231-241.
[11] G.F. Rush, J.R. Gorski, M.G. Ripple, J. Sowinski, P. Bugelski, W.R. Hewitt, Organic Hydroperoxide-Induced Lipid-Peroxidation and Cell-Death in Isolated Hepatocytes, Toxicol Appl Pharm 78(3) (1985) 473-483.
[12] A. Lagunin, A. Stepanchikova, D. Filimonov, V. Poroikov, PASS: prediction of activity spectra for biologically active substances, Bioinformatics 16(8) (2000) 747-748.
[13] A. Kamal, K.S. Reddy, M.N.A. Khan, R.V.C.R.N.C. Shetti, M.J. Ramaiah, S.N.C.V.L. Pushpavalli, C. Srinivas, M. Pal-Bhadra, M. Chourasia, G.N. Sastry, A. Juvekar, S. Zingde, M. Barkume, Synthesis, DNA-binding ability and anticancer activity of benzothiazole/benzoxazole-pyrrolo[2,1-c][1,4]benzodiazepine conjugates, Bioorgan Med Chem 18(13) (2010) 4747-4761.
[14] D. Kumar, M.R. Jacob, M.B. Reynolds, S.M. Kerwin, Synthesis and evaluation of anticancer benzoxazoles and benzimidazoles related to UK-1, Bioorgan Med Chem 10(12) (2002) 3997-4004.
[15] C.T. Zeyrek, H. Unver, O.T. Arpaci, K. Polat, N.O. Iskeleli, M. Yildiz, Experimental and theoretical characterization of the 2-(4-bromobenzyl)-5-ethylsulphonyl-1,3-benzoxazole, J Mol Struct 1081 (2015) 22-37.
[16] M.S. Ober, Froese, R. D., Quinoline-benzoxazole derived compounds for electronic films and devices, in: D.G.T. Llc (Ed.) 2014.
[17] Y. Kawata, Kadoma, H., Ohsawa, N., Seo, S. , Benzoxazole derivative, light-emitting element, light-emitting device, electronic device, and lighting device, in: L. Semiconductor Energy Laboratory Co. (Ed.) 2013.
[18] M. J. Frisch, G. W. Trucks, H. B. Schlegel, G. E. Scuseria, M. A. Robb, J. R. Cheeseman, G. Scalmani, V. Barone, B. Mennucci, G. A. Petersson, H. Nakatsuji, M. Caricato, X. Li, H. P. Hratchian, A. F. Izmaylov, J. Bloino, G. Zheng, J. L. Sonnenberg, M. Hada, M. Ehara, K. Toyota, R. Fukuda, J. Hasegawa, M. Ishida, T. Nakajima, Y. Honda, O. Kitao, H. Nakai, T. Vreven, J. A. Montgomery, J.E.P. Jr., F. Ogliaro, M. Bearpark, J. J. Heyd, E. Brothers, K. N. Kudin, V. N. Staroverov, R. Kobayashi, J. Normand, K. Raghavachari, A. Rendell, J. C. Burant, S. S. Iyengar, J. Tomasi, M. Cossi, N. Rega, J. M. Millam, M. Klene, J. E. Knox, J. B. Cross, V. Bakken, C. Adamo, J. Jaramillo, R. Gomperts, R. E. Stratmann, O. Yazyev, A. J. Austin, R. Cammi, C. Pomelli, J. W. Ochterski, R. L. Martin, K. Morokuma, V. G. Zakrzewski, G. A. Voth, P. Salvador, J. J. Dannenberg, S. Dapprich, A. D. Daniels, Ö. Farkas, J. B. Foresman, J. V. Ortiz, J. Cioslowski, D.J. Fox, Gaussian 09, Revision D.01, Gaussian, Inc., Wallingford CT, 2009.
[19] R. Dennington, T. Keith, J. Millam, GaussView, Version 5, Semichem, Inc., Shawnee Mission, KS, 2009.
[20] F.F. Charlotte, General Hartree-Fock program, Computer Physics Communications 43(3) (1987) 355-365.
[21] G.A. Petersson, A. Bennett, T.G. Tensfeldt, M.A. Allaham, W.A. Shirley, J. Mantzaris, A Complete Basis Set Model Chemistry .1. The Total Energies of Closed-Shell Atoms and Hydrides of the 1st-Row Elements, J Chem Phys 89(4) (1988) 2193-2218.
[22] T. Clark, J. Chandrasekhar, G.W. Spitznagel, P.V. Schleyer, Efficient Diffuse Function-Augmented Basis Sets for Anion Calculations. Iii. The 3-21+G Basis Set for First-Row Elements, Li-F, J Comput Chem 4(3) (1983) 294-301.
[23] P.P. G. Fogarasi, Ab initio calculation of force fields and vibrational spectra, Vibrational Spectra and Structure: a Series of Advances, vol. 14 (Chapter 3), 125–219, Elsevier, Amsterdam, 1985.

[24] SQM, SQM version 1.0, Scaled Quantum Mechanical, Green Acres Road, Fayetteville, Arkansas, 72703., 2013.
[25] R. Ditchfie, Molecular-Orbital Theories of Nmr Chemical-Shifts, Chem Phys Lett 15(2) (1972) 203.
[26] T. Koopmans, Ordering of wave functions and eigenenergies to the individual electrons of an atom, Physica 1 (1933) 104-103.
[27] E.D. Glendening, J.K. Badenhoop, A.E. Reed, J.E. Carpenter, F. Weinhold, NBO Version 3.1 Theoretical Chemistry Institute, University of Wisconsin, Madison, 1995.
[28] H.R. Drew, R.M. Wing, T. Takano, C. Broka, S. Tanaka, K. Itakura, R.E. Dickerson, Structure of a B-DNA Dodecamer - Conformation and Dynamics .1., P Natl Acad Sci-Biol 78(4) (1981) 2179-2183.
[29] O. Trott, A.J. Olson, Software News and Update AutoDock Vina: Improving the Speed and Accuracy of Docking with a New Scoring Function, Efficient Optimization, and Multithreading, J Comput Chem 31(2) (2010) 455-461.
[30] W.L. DeLano, The PyMOL Molecular Graphics System, San Carlos, CA, USA, 2016.
[31] Accelrys Software Inc Discovery Studio Modelling Environment Relaser 4.0, Accelrys Software Inc, SanDiego, 2013.
[32] M. Takasuka, H. Nakai, IR and Raman spectral and X-ray structural studies of polymorphic forms of sulfamethoxazole, Vib Spectrosc 25(2) (2001) 197-204.
[33] C. Chatterjee, J.K. Dattagupta, N.N. Saha, N-1-(3,4-Dimethyl-5-Isoxazolyl)Sulfanilamide (Sulfisoxazole), Acta Crystallogr B 38(Jun) (1982) 1845-1847.
[34] M. Ghosh, A.K. Basak, S.K. Mazumdar, B. Sheldrick, Structure and Conformation of the 1-1 Molecular-Complex Sulfaproxyline-Caffeine, Acta Crystallogr C 47 (1991) 577-580.
[35] T.P. Singh, U. Patel, M. Haridas, Structure of 2-[4-(Acetylaminosulphonyl)Phenylcarbamoyl]Benzoic Acid (Phthalylsulfacetamide), C16h14n2o6s, Acta Crystallogr C 40(Dec) (1984) 2088-2091.
[36] V.L. Abramenko, V.S. Sergienko, Molecular complexes and chelates of dioxomolybdenum(VI) with salicylidene-4-iminobenzenesulfonamides: The crystal structures of salicylidene-4-iminobenzenesulfonamido-5-ethyl-1,3,4-thiadiazole (L-5) and its MoO2L25 complex, Russ J Inorg Chem+ 47(6) (2002) 806-815.
[37] A. Kalman, M. Czugler, G. Argay, Conformational Characteristics of Anhydrous Sulfaguanidine - Computer Retrieval and Analysis of N-Substituted Arylsulfonamides, Acta Crystallogr B 37(Apr) (1981) 868-877.
[38] Ö.K. M. Yıldız, C. T. Zeyrek, B. Boyacıoglu, H. Dal,, N.Y. N. Demir, H. Ünver, Synthesis, biological activity, DNA binding and anion sensors, molecular structure and quantum chemical studies of a novel bidentate Schiff base derived from 3,5-bis(triflouromethyl)aniline and salicylaldehyde, J Mol Struct 1094 (2015) 148-160.
[39] C.T. Zeyrek, N. Dilek, M. Yildiz, H. Unver, Synthesis, structure, spectroscopic (FT-IR) and density functional modelling studies of 1-[(4-ethoxyphenylimino)methyl]napthalene-2-ol, Mol Phys 112(19) (2014) 2557-2574.
[40] C.T. Zeyrek, Theoretical Study of the N-(2,5-Methylphenyl)salicylaldimine Schiff Base Ligand: Atomic Charges, Molecular Electrostatic Potential, Nonlinear Optical (NLO) Effects and Thermodynamic Properties, J. Korean Chem. Soc. 57(4) (2013) 461-471.
[41] E. Kendi, S. Ozbey, O. Bozdag, R. Ertan, Flavone-3 '-sulfonamide, Acta Crystallogr C 56 (2000) 457-458.
[42] K. Sarojini, H. Krishnan, C.C. Kanakam, S. Muthu, Synthesis, X-ray structural, characterization, NBO and HOMO-LUMO analysis using DFT study of 4-methyl-N-(naphthalene-1-yl)benzene sulfonamide, Spectrochim Acta A 96 (2012) 657-667.
[43] S. Ozbey, A. Akbas, G. Ayhan-Kilcigil, R. Ertan, Antibacterial 4-amino-N-(5-methylisoxazol-3-yl)-N-[(4-oxo-2-phenyl-4H-1-benzopyran-6-yl)methyl]benzenesulfonamide, Acta Crystallogr C 61 (2005) O559-O561.
[44] C.N. Sundaresan, S. Dixit, P. Venugopalan, A supramolecular assembly dominated by N-H center dot center dot center dot S hydrogen bonds: Structure of 2-thioureidobenzoxazole by single crystal X-ray diffraction, J Mol Struct 693(1-3) (2004) 205-209.
[45] H. Unver, O.T. Arpaci, D.M. Zengin, T.N. Durlu, Crystal structure, spectroscopic studies and conformational analyses of 5-chloro-6-nitro-2-cyclohexylmethylbenzoxazole, J Mol Struct 609(1-3) (2002) 205-212.
[46] S.M. Lee, H.M. Ali, K.M. Lo, [N '-(5-Bromo-2-oxidobenzylidene-kappa O)-3-hydroxy-2-naphthohydrazidato-kappa N-2 ',O]dimethyltin(IV), Acta Crystallogr E 66 (2010) M161-U706.
[47] A.E.H. Machado, J.A. de Miranda, S. Guilardi, D.E. Nicodem, D. Severino, Photophysics and spectroscopic properties of 3-benzoxazol-2-yl-chromen-2-one, Spectrochim Acta A 59(2) (2003) 345-355.
[48] R.M. Silverstein, Webster, F. X., Spectroscopic identification of organic compound, 6th ed., John Willey & Sons, New York, 2003.
[49] K. Pihlaja, E. Kleinpeter, E., Carbon-13 Chemical Shifts in Structural and Sterochemical Analysis, VCH Publishers, Deerfield Beach, 1994.
[50] K.H. O., S. Berger, S. Braun, Carbon-13 NMR Spectroscopy, John Wiley & Sons, Chichester, 1988.
[51] N.P.G. Roeges, A Guide to the Complete Interpretation of IR Spectra of Organic Compounds, Wiley, New York, 1994.
[52] N.B. Colthup, L.H. Daly, S.E. Wiberly, Introduction to Infrared and Raman Spectroscopy, third ed., Academic Press, Boston, 1990.
[53] P.L. Anto, C.Y. Panicker, H.T. Varghese, D. Philip, O. Temiz-Arpaci, B. Tekiner-Gulbas, I. Yildiz, Vibrational spectroscopic studies and ab initio calculations of 5-methyl-2-(p-fluorophenyl)benzoxazole, Spectrochim Acta A 67(3-4) (2007) 744-749.

[54] T.D. Klots, W.B. Collier, Heteroatom Derivatives of Indene .3. Vibrational-Spectra of Benzoxazole, Benzofuran, and Indole, Spectrochim Acta A 51(8) (1995) 1291-1316.
[55] Shana Parveen S, Monirah. A. Al-Alshaikh, C. Yohannan Panicker, Ali A. El-Emam, Mustafa Arisoy, Ozlem Temiz-Arpaci, C.V. Alsenoy, Synthesis, vibrational spectroscopic investigations, molecular docking, antibacterial and antimicrobial studies of 5-ethylsulphonyl-2-(p-aminophenyl)benzoxazole, J Mol Struct 1115 (2016) 94-104.
[56] Y.S. Mary, K. Raju, T.E. Bolelli, I. Yildiz, H.I.S. Nogueira, C.M. Granadeiro, C. Van Alseony, FT-IR, FT-Raman, surface enhanced Raman scattering and computational study of 2-(p-fluorobenzyl)-6-nitrobenzoxazole, J Mol Struct 1012 (2012) 22-30.
[57] B.C. Smith, Infrared spectral interpretation, a systematic approach, CRC Press, New York, 1999.
[58] C. Andraud, T. Brotin, C. Garcia, F. Pelle, P. Goldner, B. Bigot, A. Collet, Theoretical and Experimental Investigations of the Nonlinear-Optical Properties of Vanillin, Polyenovanillin, and Bisvanillin Derivatives, J Am Chem Soc 116(5) (1994) 2094-2102.
[59] C. Adant, M. Dupuis, J.L. Bredas, Ab-Initio Study of the Nonlinear-Optical Properties of Urea - Electron Correlation and Dispersion Effects, Int J Quantum Chem (1995) 497-507.
[60] Y.S. Mary, K. Raju, I. Yildiz, O. Temiz-Arpaci, H.I.S. Nogueira, C.M. Granadeiro, C. Van Alsenoy, FT-IR, FT-Raman, SERS and computational study of 5-ethylsulphonyl-2-(o-chlorobenzyl)benzoxazole, Spectrochim Acta A 96 (2012) 617-625.
[61] J.B. Bhagyasree, H.T. Varghese, C.Y. Panicker, J. Samuel, C. Van Alsenoy, K. Bolelli, I. Yildiz, E. Aki, Vibrational spectroscopic (FT-IR, FT-Raman, H-1 NMR and UV) investigations and computational study of 5-nitro-2-(4-nitrobenzyl) benzoxazole, Spectrochim Acta A 102 (2013) 99-113.
[62] S. Muthu, G. Ramachandran, E.I. Paulraj, T. Swaminathan, Quantum mechanical study of the structure and spectroscopic (FTIR, FT-Raman), first-order hyperpolarizability and NBO analysis of 1,2-benzoxazol-3-ylmenthane sulfonamide, Spectrochimica Acta Part a-Molecular and Biomolecular Spectroscopy 128 (2014) 603-613.
[63] S.M. Rida, F.A. Ashour, S.A.M. El-Hawash, M.M. Elsemary, M.H. Badr, M.A. Shalaby, Synthesis of some novel benzoxazole derivatives as anticancer, anti-HIV-1 and antimicrobial agents, Eur J Med Chem 40(9) (2005) 949-959.
[64] B. Kramer, M. Rarey, T. Lengauer, Evaluation of the FLEXX incremental construction algorithm for protein-ligand docking, Proteins 37(2) (1999) 228-241.

The figures captions:

Scheme 1. The synthesis diagrams of the compound.

Figure 1. The optimized geometry of the compound.

Figure 2. (a) ^{1}H (b) ^{13}C NMR spectrum of the title compound and (c) HSQC spectra for the aromatic region of the compound.

Figure 3. FT-IR spectrum of the investigated compound.

Figure 4. Molecular orbital surfaces and energy levels given in parentheses for the HOMO – 1, HOMO, LUMO, and LUMO +1 of the title compound computed at 6-311++G(d,p) level.

Figure 5. (a) Co-crystallized molecule shown in yellow color and the docked conformation of **L** (blue) as predicted by the Autodock Vina show very low RMSD value. (b) Representation of docking results of **L** embedded into the NADPH. (For interpretation of the references to colour in this figure legend, the reader is referred to web version of this article).

Figure 6. (a) The ligand binds at the active site of NADPH. (b) 5-ethylsulphonyl-2-(p-ethylphenyl)-benzoxazole and NADPH interaction (2D).

Figure 7. (a) Docked poses of **L** with B-DNA. (b) Binding interactions of **L** with B-DNA at the active site residues.

Supplementary material

Figure S1. Molecular electrostatic potential (MEP) map calculated at B3LYP/6-311++G(d,p) level.

Table 1 Optimized structural parameters using HF and DFT/B3LYP with 6-311++G(d,p) basis set of the title compound in the ground state. Bond distances (*Å*) and angles (*°*) with e.s.d.s in parentheses.

Parameters	B3LYP/6-311++G(d,p)	HF/6-311++G(d,p)	Selected Similar parameter[a]
Bond distances (Å)			
S1-O2	1.469	1.433	1.435(2)[b], 1.433(2)[d], 1.44(1)[e], 1.445(2)[f], 1.437(2)[k]
S1-C3	1.806	1.773	1.747(3)[b], 1.78(1)[e], 1.767(2)[f], 1.768(2)[k]
S1-O3	1.469	1.433	1.427(2)[b], 1.427(3)[d], 1.42(1)[e], 1.441(2)[f], 1.429(2)[k]
S1-C2	1.827	1.788	1.758(3)[k]
O1-C6	1.365	1.348	1.386(2)[g], 1.375(4)[h], 1.373(3)[k]
O1-C9	1.385	1.351	1.359(2)[g], 1.380(5)[h], 1.380(3)[k]
C5-C6	1.402	1.382	1.379(2)[g], 1.387(3)[i], 1.381(3)[k]
C6-C7	1.385	1.378	1.376(2)[g], 1.362(5)[h], 1.364(2)[k], 1.370(3)[l], 1.371(3)[i]
N1-C5	1.389	1.388	1.409(2)[g], 1.396(5)[h], 1.409(3)[k],
N1-C9	1.297	1.271	1.289(2)[g], 1.288(5)[h], 1.296(3)[i], 1.283(3)[k]
C3-C4	1.393	1.385	1.376(4)[b], 1.388(3)[k]
C3-C8	1.405	1.398	1.372(4)[b], 1.387(3)[k]
C12-C13	1.402	1.393	1.359(4)[k]
C13-C14	1.400	1.389	1.364(4)[k]
C4-C5	1.394	1.383	1.385(2)[g]
C9-C10	1.456	1.465	1.472(5)[h], 1.461(3)[i], 1.481(3)[k]
C10-C11	1.403	1.391	1.375(4)[k]
C10-C15	1.401	1.388	1.370(4)[k]
C7-C8	1.393	1.383	1.378(3)[k]
C11-C12	1.388	1.380	1.376(4)[k]
C1-C2	1.522	1.523	1.501(4)[4]
C14-C15	1.390	1.384	1.381(4)[k]
C16-C17	1.540	1.534	
Bond angles (°)			
O2-S1-C3	107.65	107.81	107.7(1)[k]
O2-S1-O3	120.99	120.09	118.86(12)[b], 120.1(1)[c], 118.89(16)[d], 118.1(7)[e], 118.7(1)[k]
O2-S1-C2	107.80	107.90	108.4(1)[k]
C3-S1-O3	107.75	107.91	108.05(13)b, 107.2(1)[c], 109.70(17)[d], 109.3(7)[e], 107.0(2)[f], 108.4(1)[k]
C3-S1-C2	105.15	105.96	107.7(1)[k]
O3-S1-C2	106.46	106.34	108.4(1)[k]
C6-O1-C9	104.46	105.10	102.85(12)[g], 104.0(3)[h], 104.3(2)[i], 104.2(2)[k]
O1-C6-C5	107.44	107.12	107.3(3)[h], 107.2(2)[i], 107.8(2)[k]
O1-C6-C7	128.48	128.75	127.7(16)[g], 128.5(4)[h], 129.1(2)[i], 128.4(2)[k]
C5-C6-C7	124.08	124.13	123.8(2)[k]
C5-N1-C9	104.96	104.68	103.06(13)[g], 104.3(3)[h], 104.3(2)[i], 104.7(2)
S1-C3-C4	118.57	118.85	120.8(2)[b], 120.6(12)[e], 119.6(2)[k]
S1-C3-C8	118.27	118.51	118.15(2)[k]
C4-C3-C8	123.15	122.64	122.2(2)[k]
C12-C13-C14	118.09	118.26	120.6(3)[k]
C12-C13-C16	120.94	120.77	
C14-C13-C16	120.95	120.95	
C3-C4-C5	116.36	116.49	116.3(2)[k]
C9-C10-C11	119.39	119.38	
C9-C10-C15	121.42	121.25	
C11-C10-C15	119.18	119.37	117.6(3)[k]
C6-C5-N1	108.68	108.16	108.84(14)[g], 109.3(3)[h], 108.9(2)[i], 108.4(2)[k]
C6-C5-C4	119.96	120.21	120.08(16)[g], 120.5(2)[k]
N1-C5-C4	131.36	131.63	131.08(16)[g], 130.7(4)[h], 131.2(2)[i], 131.1(2)[k]
O1-C9-N1	114.46	114.94	117.29(14)[g], 115.1(3)[h], 115.3(2)[i], 114.9(2)[k]
O1-C9-C10	117.37	117.42	116.0(4)[g]
N1-C9-C10	128.18	127.64	128.9(4)[g]
C6-C7-C8	115.91	115.80	115.8(2)[k]
C13-C12-C11	121.29	121.12	119.3(3)[k]
S1-C2-C1	114.25	114.82	114.4(2)[k]
C13-C14-C15	121.27	121.08	119.3(3)[k]
C3-C8-C7	120.54	120.73	121.4(2)[k]
C10-C11-C12	120.09	120.07	121.7(3)[k]
C10-C15-C14	120.08	120.09	119.3(3)[k]
C13-C16-C17	112.82	112.81	
Selected torsion angles (°)			
O2-S1-C3-C4	-18.72	-19.07	-18.4(2) [k]
O2-S1-C3-C8	160.77	160.87	162.7(2)[k]
O3-S1-C3-C4	-150.73	-150.17	-148.0(2)[k]
O3-S1-C3-C8	28.77	29.77	33.2(2)[k]
C2-S1-C3-C4	96.02	96.25	96.6(2)[k]
C2-S1-C3-C8	-84.49	-83.81	-82.3(2)[k]
O2-S1-C2-C1	47.19	48.63	52.0(3)[k]
C3-S1-C2-C1	-67.44	-66.63	-63.5(3)[k]
O3-S1-C2-C1	178.39	178.71	-178.4(2)[k]
C9-O1-C6-C5	0.08	0.05	-0.6(2)[k]
C6-O1-C9-N1	-0.06	-0.03	1.0(3)[k]
S1-C3-C4-C5	-179.80	-179.19	-176.9(2)[k]
C11-C10-C9-N1	0.33	0.10	

C15-C10-C9-O1	0.53	0.25
C9-C10-C11-C12	179.99	-179.90
C12-C13-C16-C17	89.11	87.44
C14-C13-C16-C17	-89.21	-91.27

[a] Similar experimental geometrical parameter in the literature.
[b] Ref. [42] (Sarojini *et. al.)*
[c] Ref. [41] (Kendi et. al)
[d] Ref. [43] (Özbey, *et. al.*)
[e] Ref. [35] (Singh *et. al.*)
[f] Ref. [37] (Kalman *et. al.*)
[g] Ref. [44] (Sundaresan *et. al.*)
[h] Ref. [45] (Ünver *et. al.*)
[i] Ref. [47] (Machado *et. al.*)
[k] Ref. [15] (Zeyrek *et. al.*)

Table 2 Experimental and theoretical [B3LYP/6-311++G(d,p)] ^{1}H and ^{13}C NMR data of the titled compound (δ in ppm, J in Hz, s: singlet, d: doublet, t: triplet, and q: quartet peak).

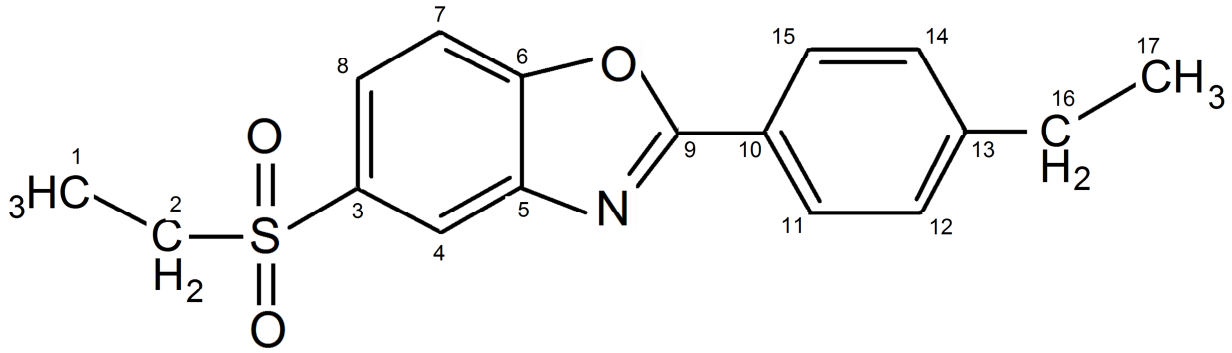

Nucleus	Experimental (in $CDCl_3$)	Theoretical (in gas)	Theoretical (in $CDCl_3$)	Nucleus	Experimental (in $CDCl_3$)	Theoretical (in gas)	Theoretical (in $CDCl_3$)
$\boldsymbol{H}_1$	1.30(t,3H)	1.51(a), 0.87(b), 0.60 (c)	1.42(a), 1.06(b), 0.69 (c)	$\boldsymbol{C}_1$	7.61	8.86	8.83
$\boldsymbol{H}_2$	3.17(q,2H)	2.72(a), 2.88(b)	2.96(a), 3.07(b)	$\boldsymbol{C}_2$	51.02	61.02	62.21
$\boldsymbol{H}_4$	8.31(s,1H)	8.28	8.21	$\boldsymbol{C}_3$	135.10	146.26	145.43
$\boldsymbol{H}_7$	7.73(d,1H)	7.62	7.84	$\boldsymbol{C}_4$	120.80	126.60	125.57
$\boldsymbol{H}_8$	7.91(d,1H)	7.90	7.92	$\boldsymbol{C}_5$	142.84	148.66	148.48
$\boldsymbol{H}_{11}$,$\boldsymbol{H}_{15}$	8.18(q,2H)	8.73, 8.36	8.70, 8.43	$\boldsymbol{C}_6$	153.73	159.21	159.86
$\boldsymbol{H}_{12}$,$\boldsymbol{H}_{14}$	7.39 (d,2H)	7.48, 7.45	7.62, 7.61	$\boldsymbol{C}_7$	111.23	113.78	115.17
$\boldsymbol{H}_{16}$	3.68(q,2H)	2.61(a), 2.62(b)	2.69(a), 2.70(b)	$\boldsymbol{C}_8$	125.08	128.60	128.72
$\boldsymbol{H}_{17}$	1.32(t,1H)	1.38(a), 1.09(b), 1.07(c)	1.42(a), 1.08(b), 1.07(c)	$\boldsymbol{C}_9$	165.65	171.18	172.16
$^{3}J_{7\text{-}8}$	8.3			$\boldsymbol{C}_{10}$	123.57	129.36	128.59
$^{3}J_{11\text{-}12}$, $^{3}J_{14\text{-}15}$	8.2			$\boldsymbol{C}_{11}$,$\boldsymbol{C}_{15}$	128.12	134.90, 132.42	134.36, 132.68
$^{3}J_{1\text{-}2,}$ $^{3}J_{16\text{-}17,}$	7.6			$\boldsymbol{C}_{13}$	149.50	157.04	158.69
				$\boldsymbol{C}_{12}$,$\boldsymbol{C}_{14}$	128.68	133.62, 133.03	134.07, 133.74
				$\boldsymbol{C}_{16}$	20.02	34.52	34.26
				$\boldsymbol{C}_{17}$	15.17	19.47	19.25

Table 3 The calculated wavenumbers, observed FT-IR bands and assignments of the title compound.

Assignments (% PED)[a]	Experiment[b] (cm^{-1})	B3LYP/ 6-311++G(d,p) (unscaled) (cm^{-1})	B3LYP/ 6-311++G(d,p) (scaled)[c] (cm^{-1})	Mode
$\upsilon_s(CH)_{PhII}(99)$		3214	3106	111
$\upsilon_s(CH)_{PhII}(98)$		3209	3101	110
$\upsilon_s(CH)_{PhI}$ (94)		3201	3093	109
$\upsilon_{as}(CH)_{PhI}(96)$		3200	3092	108
$\upsilon_{as}(CH)_{PhII}(100)$		3197	3089	107
$\upsilon_{as}(CH)_{PhI}(99)$	3052	3164	3058	106
$\upsilon_{as}(CH)_{PhI}(100)$		3162	3056	105
$\upsilon_{as}(CH_2)(37)+\upsilon_{as}(CH_3)(61)$		3128	3023	104
$\upsilon_{as}(CH_2)(57)+\upsilon_{as}(CH_3)(43)$		3109	3005	103
$\upsilon_{as}(CH_2)(8)+\upsilon_{as}(CH_3)(92)$		3101	2996	102
υ_{as} $(CH_2)(12)+\upsilon_{as}(CH_3)(88)$		3098	2993	101
$\upsilon_{as}(CH_3)(99)$		3093	2999	100
υ_{as} $(CH_2)(87)+\upsilon_{as}(CH_3)(12)$		3061	2958	99
$\upsilon_s(CH_2)(97)$	2969	3061	2958	98
$\upsilon_s(CH_3)(100)$		3040	2938	97
$\upsilon_s(CH_2)(95)+\upsilon_s(CH_3)(4)$		3030	2928	96
$\upsilon_s(CH_3)(96)$	2925	3026	2925	95
$\upsilon(PhII)_{ring}$ (7)+υ(N=C)(7)+$\upsilon(PhI)_{ring}(42)+\upsilon$(C–C)(6)	1620	1654	1617	94
$\upsilon(PhII)_{ring}$ (34)+υ(N=C)(8)+$\upsilon(PhI)_{ring}(24)$		1647	1610	93
$\upsilon(PhII)_{ring}$ (59)+υ(N=C)(5)	1596	1637	1600	92
$\upsilon(PhII)_{ring}$ (13)+$\upsilon(PhI)_{ring}(48)$		1606	1570	91
υ(N=C)(22)+υ(C–C)(13)+$\upsilon(PhII)_{ring}(7)+\upsilon(PhI)_{ring}(20)$	1553	1585	1550	90
υ(N=C)(13)+υ(PhI)ring(21)+$\rho(CH)_{PhI}(47)$		1533	1503	89
$\delta_{as}(CH_3)(33)+\delta_s(CH_2)(7)+\tau$(H-C16-C17-C13)(7)+$\tau$(H-C16-C17-H)(22)		1509	1492	88
$\delta_{as}(CH_3)(63)+\tau$(H-C2-C1-H)(22)+$\tau$(H-C2-C1-S1)(10)		1506	1492	87
$\delta_{as}(CH_3)(52)$		1497	1483	86
$\delta_{as}(CH_3)(53)$	1455	1495	1481	85
sci$(CH_2)(29)$		1491	1472	84
$\upsilon(PhII)_{ring}(27)+\rho(CH)_{PhII}(42)$		1481	1454	83
sci$(CH_2)(29)$		1456	1438	82
υ(N-C)(8)+$\upsilon(PhII)_{ring}(32)+\rho(CH)_{PhII}(16)$	1415	1454	1425	81
$\upsilon(PhI)_{ring}(23)+\rho(CH)_{PhI}(30)$		1446	1419	80

$\delta_s(CH_3)(40)$		1417	1405	79
$\delta_s(CH_3)(52)$		1411	1401	78
$\upsilon(N=C)(4)+\upsilon(PhII)_{ring}(59)$		1379	1347	77
$\upsilon(PhI)_{ring}(13)+t(CH_2)(8)+\rho(CH)_{PhI}(61)$		1354	1328	76
$w(CH_2)(72)+\rho(CH)_{PhI}(61)$		1351	1327	75
$\upsilon(PhI)_{ring}(44)+\rho(CH)_{PhI}(12)$	1306	1342	1314	74
$\upsilon_{as}(SO_2)(5)+\gamma(CH_2–S)(23)+\gamma(CH_2–CH_3)(22)$		1313	1288	73
$\upsilon(N=C)(11)+\upsilon(C–O)(12)+\upsilon(PhI)_{ring}(18)+\rho(CH)_{PhII}(12)+\upsilon(PhII)_{ring}(5)$		1306	1277	72
$\upsilon(C–O)(4)+\upsilon(PhII)_{ring}(13)+\rho(CH)_{PhII}(61)$	1279	1282	1259	71
$\upsilon_{as}(S–O)(10)+\gamma(CH_2–S)(17)+\gamma(CH_2–CH_3)(45)$		1271	1248	70
$\upsilon(PhI)_{ring}(12)+\gamma(CH_2–CH_3)(49)$	1259	1270	1247	69
$\upsilon(C–N)(38)+\upsilon(PhII)ring(12)+\rho(CH)_{PhII}(17)$		1258	1230	68
$\upsilon_{as}(S–O)(73)+\gamma(CH_2–CH_3)(8)$	1243	1255	1226	67
$\upsilon(C–O)(6)+\upsilon(C–C)(28)+\upsilon(PhI)_{ring}(9)+\rho(CH)_{PhI}(13)$		1227	1202	66
$\upsilon(C–O)(16)+\upsilon(N=C)(4)+\upsilon(PhII)_{ring}(4)+\rho(CH)_{PhI}(16)$		1219	1193	65
$\rho(CH)_{PhI}(68)$		1204	1181	64
$\upsilon(PhI)_{ring}(27)+\rho(CH)_{PhI}(54)$	1132	1145	1124	63
$\upsilon(PhII)_{ring}(22)+\rho(CH)_{PhII}(52)$		1143	1122	62
$\upsilon_s(S–O)(40)+\upsilon_{as}(S–C_{phII})(6)$	1042	1103	1077	61
$\upsilon(CH_2–CH_3)(16)+\gamma(CH_2–CH_3)(51)$		1079	1059	60
$\upsilon(CH_2–CH_3)(34)+\gamma(CH_2–CH_3)(34)$		1078	1055	59
$\upsilon(PhI)_{ring}(15)+\delta(CCH)(34)+\tau(HCCH)(18)$		1071	1050	58
$\upsilon(C9–O)(9)+\upsilon(PhI)_{ring}(17)+\upsilon(PhII)_{ring}(7)+\rho(N1\text{-}C9\text{-}O1)(4)$		1061	1039	57
$\upsilon_s(S–O)(22)+\upsilon(C–O1)(5)+\delta(H\text{-}C2\text{-}S1)(12)+\delta(H\text{-}C2\text{-}C1)(13))+\tau(H\text{-}C1\text{-}C2\text{-}H)(12)$		1056	1034	56
$\upsilon_s(S–O)(24)+\upsilon(S\text{-}C3)(3)+\upsilon(PhII)_{ring}(28)+\delta(HCC)_{PhII}(14)$		1051	1028	55
$\upsilon(PhI)_{ring}(16)+\rho(CH)_{PhI}(24)+\rho(C\text{-}C\text{-}C)_{phI}(35)$		1032	1018	54
$\tau(PhI)(83)$		995	977	53
$\upsilon(C1\text{-}C2)(53)+\upsilon(C2\text{-}S)(4)+\delta(H\text{-}C1\text{-}C2)(11)$		985	961	52
$\tau(PhI)(82)$		979	960	51
$\upsilon(C17\text{-}C16)(69)+\delta(H\text{-}C17\text{-}C16)(8)$		970	946	50
$\tau(PhII)(88)$		960	942	49
$\upsilon(C\text{-}N)(9)+\upsilon(C6\text{-}O1)(4)+\upsilon(PhII)_{ring}(28)+\upsilon(C3\text{-}S1)(6)+\delta(C6\text{-}O1\text{-}C9)(9)+\delta(HCC)_{phII}(9)$		935	922	48
$\upsilon(C\text{-}N)(5)+\upsilon(C9\text{-}O1)(37)+\upsilon(PhII)_{ring}(12)+\delta(C6\text{-}O1\text{-}C9)(6)+\rho(O1\text{-}C9\text{-}N1)(7)+\rho(C5\text{-}N1\text{-}C9)(8)$		934	917	47
$\tau(PhII)_{ring}(86)$		918	904	46
$\tau(PhI)_{ring}(77)$		861	848	45

$\tau(PhI)_{ring}(89)$		853	840	44
$\upsilon(C6\text{-}O1)(14)+\upsilon(C5\text{-}N)(3)+\upsilon(PhII)_{ring}(20)+\upsilon(PhI)_{ring}(6)+\delta(HCC)_{PhII}(6)+\delta(C5\text{-}N1\text{-}C9)(3)$		841	823	43
$\tau(PhII)_{ring}(85)$	808	825	813	42
$\delta(H\text{-}C16\text{-}C17)(42)+\tau(CH_2\text{-}CH_3)_{PhI}(53)$		795	781	41
$\upsilon(PhI)_{ring}(34)+\delta(PhI)_{ring}(9)$	784	790	776	40
$\gamma(CH_2\text{–}CH_3)(33)+\tau(H\text{-}C2\text{-}S\text{-}O3)(20)+\tau(H\text{-}C2\text{-}S\text{-}C3)(6))+\tau(CH_2\text{-}CH_3)_{PhII}(26)$		785	771	39
$\tau(N\text{-}C5\text{-}C6\text{-}O1)(4)+\tau(PhI)_{ring}(18)+)+\tau(HCCC)_{PhII}(14)+\tau(O1\text{-}C9\text{-}N\text{-}C5)(6)+\tau(C6\text{-}C5\text{-}N\text{-}C9)(10)$		765	753	38
$\tau(N\text{-}C5\text{-}C6\text{-}O1)(7)+\tau(N1\text{-}C9\text{-}C10\text{-}C11)(6)+\tau(PhI)_{ring}(23)+\tau(C5\text{-}C6\text{-}O1\text{-}C9)(4)+\tau(O1\text{-}C9\text{-}C10\text{-}C15)(5)$	740	761	750	37
$\upsilon(C3\text{-}S1)(9)+\upsilon(CH_2\text{-}S)(11)+\upsilon(PhII)_{ring}(3)+\gamma(C5\text{-}C6\text{-}O1)(6)+\gamma(C6\text{-}C5\text{-}N)(4)+\gamma(PhII)_{ring}(8)$		729	717	36
$\tau(N\text{-}C9\text{-}O1\text{-}C6)(10)+\tau(O1\text{-}C9\text{-}N\text{-}C5)(8)+\tau(O1\text{-}C9\text{-}C10\text{-}C11)(4)+\tau(N\text{-}C9\text{-}C10\text{-}C11)(3)$		720	709	35
$\upsilon(S\text{-}CH_2)(27)+\gamma(C6\text{-}C5\text{-}N)(4)+\gamma(C5\text{-}C6\text{-}O1)(5)+\gamma(C6\text{-}C5\text{-}N)(4)+\tau(CCSO)(8)$	676	678	668	34
$\upsilon(\ PhI)_{ring}(6)+\delta(PhI)_{ring}(37)+\delta(HCC)_{PhI}(14)$		651	645	33
$\upsilon(\ C\text{-}C)(21)+\delta(PhI)_{ring}(7)+\delta(PhII)_{ring}(19)$	666	642	634	32
$\upsilon(S\text{-}CH_2)(13)+\gamma(C3\text{-}S1\text{-}CH_2)(3)+\tau(N\text{-}C5\text{-}C4\text{-}C3)(3)+\tau(PhII)_{ring}(38)$	588	619	609	31
$\upsilon(C\text{-}C)(14)+\delta(O1\text{-}CC)(14)+\delta(N\text{-}CC)(6)+\delta(PhI)_{ring}(10)$		587	580	30
$\delta(PhII)_{ring}(11)+\delta(PhI)_{ring}(8)+\delta(O1\text{-}CC)(11)+\delta(N\text{-}CC)(17)$	555	559	554	29
$\upsilon(C\text{-}C)(6)+\delta(PhI)_{ring}(3)+\tau(PhII)_{ring}(25)$	535	536	529	28
$\delta(SO_2)(17)+\tau(C4\text{-}C3\text{-}S1\text{-}O2)(4)+\tau(CH_2\text{-}S1\text{-}O2)(17)+\tau(C8\text{-}C3\text{-}S1\text{-}O2)(4)+\tau(C1\text{-}C2\text{-}S1\text{-}O2)(6)$	523	511	504	27
$\upsilon(S\text{-}C2)(8)+\gamma(C3\text{-}S1\text{-}O3)(8)+\gamma(C2\text{-}S1\text{-}O3)(9)+\gamma(C1\text{-}C2\text{-}S1)(10)+\tau(C4\text{-}C3\text{-}S1\text{-}O2)(6)+\tau(C8\text{-}C3\text{-}S1\text{-}O2)(6)$	502	488	481	26
$\tau(CCCH)_{PhII}(15)+\tau(CCCC)_{PhII}(25)+\tau(CC\text{-}O1\text{-}C)(10)+\tau(CC\text{-}N1\text{-}C)(7)$	451	446	439	25
$\upsilon(S\text{-}C2)(11)+\gamma\ (O2\text{-}S\text{-}C3)(8)+\ \gamma(C4\text{-}C3\text{-}S1)(7)+\tau(C4\text{-}C3\text{-}S1\text{-}O3)(4)$	429	430	425	24
$\tau(PhI)_{ring}(90)$	417	414	408	23
$\delta(C17\text{-}C16\text{-}C13)(8)+\tau(PhII)_{ring}(34)$	409	406	400	22
$\upsilon(S\text{-}C2)(8)+\delta(PhI)_{ring}(34)+\delta(O3\text{-}S1\text{-}C2)(7)+\delta(N1\text{-}C5\text{-}C4)(3)+\ \tau(CC\text{-}S1\text{-}O3)(6)$		383	378	21
$\gamma(O2\text{-}S\text{-}O3)(5)+\gamma(C3\text{-}S\text{-}C2)(11)+\gamma(O3\text{-}S1\text{-}C2)(6)+\tau(C8\text{-}C7\text{-}C6\text{-}O1)(5)$		351	347	20
$\upsilon(S\text{-}C2)(3)+\delta(O\text{-}S1\text{-}C)(18)$		340	336	19
$\upsilon(S\text{-}C3)(17)+\ \upsilon(C9\text{-}C10)(11)+\delta(PhI)_{ring}(5)$		327	322	18
$\gamma(O2\text{-}S\text{-}C3)(9)+\ \gamma(N\text{-}C5\text{-}C4)(5)+\gamma(C7\text{-}C6\text{-}O1)(5)$		287	284	17
$\upsilon(S\text{-}C3)(6)+\tau(NCCC)(11)$		282	277	16
$\tau(CH_2\text{–}CH_3)(35)$		253	249	15

δ(O-S1-C) (12)+τ(CH_2–CH_3)(19)	220	217	14
υ(S-C3)(6)+γ(O2-S-C2)(4)+τ(O2-S-CH_2)(5)(16)	219	215	13
τ(CH_2 –CH_3)(41)	215	212	12
υ(S-C3)(6)+δ(C-S1-C)(18)	203	200	11
υ(S-C3)(4)+δ(C-C-S1)(18)+δ(C-C-C) (6)	168	166	10
δ(C-S1-C) (38)+δ(C-C-C) (12)	147	145	9
δ(C-S1-C) (8)+δ(C-C-C)(4)+τ(C10-C9-N1-C5)(5)+τ(C11-C12-C13-C16)(5)	116	114	8
τ(H-C-S1-C)(14)+τ(C-C-S1-O)(13)+τ(C-C-S1-C)(13)+τ(C-C-C-C)(11)	91	90	7
δ(O1-C9-C10) (15)+δ(N1-C9-C10) (16)+δ(C9-C10-C11) (10)+δ(C9-C10-C15)(10)	68	68	6
δ(C3-S1-C2)(8)+τ(C1-C2-S1-C3)(10)	61	60	5
τ(O1-C9-C10-C11)(22)+τ(O1-C9-C10-C15)(13)	52	51	4
τ(C17-C16-C13-C12)(14)+τ(C17-C16-C13-C14)(16)	41	41	3
τ(C4-C3-S-C2)(10)+τ(C4-C3-S-O2)(5)+τ(C8-C3-S-C2)(10)+τ(C8-C3-S-O3)(5)+τ(O1-C9-C10-C15)(7)	32	32	2
τ(N1-C9-C10-C15)(11)+τ(C10-C9-N-C5)(10)+τ(C10-C9-O1-C6)(8)	27	26	1

[a]*Abbreviations*: ν:bond stretching, δ:in-plane deformation, γ: out-of-plane deformation, sci:scissoring, t:twisting, τ:torsion, w:wagging, ρ:rocking, PhI: Para-substitued phenyl ring, PhII: trisubstitued phenyl ring, RingIII: benzoxazole ring, as:antisymmetric and s:symmetric, % of PED is given bracket for B3LYP.
[b]*vs*: very strong, *s*: strong, *m*: medium, *w*: weak, *sh*: shoulder.
[c]Scaled with quantum mechanics force field (SQMFF) methodology [17].

Table 4 Second-order perturbation theory analysis of the Fock matrix in NBO basis, calculated at B3LYP/6-311++G(d,p) level. LP for 1 center valance lone pair.

Donor orbital (*i*)	Type	Occupancy	Donor orbital (*i*)	Type	Occupancy	$E^{(2)}$(kcal/mol)[a]	$\varepsilon_i - \varepsilon_j$ (a.u.)[b]	F_{ij} (a.u.)[c]
H4 - C4	σ	1.97915	C6 - C5	σ^*	0.04090	3.26	1.06	0.053
			C3 - C8	σ^*	0.02386	3.45	1.07	0.054
H8 - C8	σ	1.98045	C3 - C4	σ^*	0.02194	3.52	1.09	0.055
H4 - C7	σ	1.98082	C6 - C5	σ^*	0.04090	3.38	1.07	0.054
H14 - C14	σ	1.98300	C13 - C12	σ^*	0.02319	3.18	1.09	0.053
			C10 - C15	σ^*	0.02194	3.18	1.09	0.053
H12 - C12	σ	1.98290	C13 - C14	σ^*	0.02306	3.17	1.09	0.053
			C10 - C11	σ^*	0.02351	3.18	1.09	0.053
H15 - C15	σ	1.98268	C13 - C14	σ^*	0.02306	3.15	1.10	0.053
			C10 - C11	σ^*	0.02351	3.39	1.09	0.054
H11 - C11	σ	1.98224	C13 - C12	σ^*	0.02319	3.20	1.09	0.053
			C10 - C15	σ^*	0.02355	3.43	1.09	0.055
H1C- C1	σ	1.98107	S1 - C2	σ^*	0.25656	4.69	0.59	0.050
S1 - O2	σ	1.98328	S1 - O3	σ^*	0.16597	3.30	1.14	0.057
S1 - C3	σ	1.97042	S1 - O2	σ^*	0.16743	3.41	0.89	0.051
			S1 - O3	σ^*	0.16597	3.47	0.90	0.052
S1 - O3	σ	1.98283	S1 - O2	σ^*	0.16743	3.23	1.13	0.056
S1 - C2	σ	1.97175	S1 - O2	σ^*	0.16743	3.39	0.87	0.050
			S1 - O3	σ^*	0.16597	3.64	0.87	0.052
O1 - C9	σ	1.99075	C6 - C7	σ^*	0.02320	4.26	1.50	0.071
C6 - C5	σ	1.97644	C6 - C7	σ^*	0.02320	5.65	1.31	0.077
			C4 - C5	σ^*	0.02685	4.65	1.31	0.070
	π	1.60828	N1 - C9	π^*	0.31863	10.58	0.27	0.049
			C3 - C4	π^*	0.35618	21.00	0.28	0.070
			C7 - C8	π^*	0.31644	17.38	0.29	0.065
C6 - C7	σ	1.97654	C6 - C5	σ^*	0.04090	5.48	1.28	0.075

N1 - C5	σ	1.97411	C10 - C9	σ^*	0.03654	5.96	1.28	0.078
N1 - C9	σ	1.98779	C4 - C5	σ^*	0.02685	4.78	1.48	0.075
	π	1.85957	C6 - C5	π^*	0.47150	15.99	0.33	0.071
			C10 - C15	π^*	0.39314	8.62	0.35	0.053
C3 - C4	σ	1.97378	N1 - C5	σ^*	0.02131	4.99	1.16	0.068
			C3 - C8	σ^*	0.02386	4.66	1.27	0.069
	π	1.72330	S1 - C2	σ^*	0.25656	4.40	0.36	0.036
			C6 - C5	π^*	0.47150	16.28	0.27	0.063
			C7 - C8	π^*	0.31644	20.69	0.29	0.069
C3 - C8	σ	1.97704	C3 - C4	σ^*	0.02194	4.77	1.29	0.070
		1.97563	C13 - C14	σ^*	0.02306	3.47	1.27	0.059
			C12 - C11	σ^*	0.01506	3.23	1.29	0.058
C13 - C14	σ	1.97564	C13 - C12	σ^*	0.02319	3.46	1.27	0.059
			C14 - C15	σ^*	0.01527	3.23	1.29	0.058
	π	1.62808	C10 - C15	π^*	0.39314	23.88	0.27	0.072
			C12 - C11	π^*	0.29477	17.89	0.28	0.064
C4- C5	σ	1.97111	S1 - C3	σ^*	0.26279	3.40	0.84	0.051
			C6 - C5	σ^*	0.04090	4.47	1.26	0.067
			C3 - C4	σ^*	0.02194	3.26	1.29	0.058
C10 - C9	σ	1.97487	C10 - C15	σ^*	0.02355	3.35	1.28	0.058
C10 - C11	σ	1.96960	C10 - C9	σ^*	0.03654	3.06	1.19	0.054
			C10 - C15	σ^*	0.02355	4.45	1.27	0.067
C10 - C15	σ	1.97262	C10 - C11	σ^*	0.02351	4.48	1.27	0.067
	π	1.63579	N1 - C9	π^*	0.31863	24.38	0.24	0.069
			C13 - C14	π^*	0.33520	17.95	0.28	0.064
			C12 - C11	π^*	0.29477	20.08	0.28	0.068
C7 - C8	σ	1.96896	S1 - C3	σ^*	0.26279	3.03	0.83	0.048
			O1 - C6	σ^*	0.03002	6.37	1.02	0.072
			C6 - C7	σ^*	0.02320	3.29	1.29	0.058
			C3 - C8	σ^*	0.02386	3.41	1.25	0.059

	π	1.69288	C6 - C5	π^*	0.47150	22.50	0.26	0.072
			C3 - C4	π^*	0.35618	17.87	0.27	0.063
C12 - C11	σ	1.97828	C13 - C12	σ^*	0.02319	3.48	1.28	0.060
			C10 - C9	σ^*	0.03654	3.04	1.19	0.054
			C10 - C11	σ^*	0.02351	3.42	1.27	0.059
	π	1.67165	C13 - C14	π^*	0.33520	21.71	0.28	0.070
			C10 - C15	π^*	0.39314	18.60	0.27	0.065
C14 - C15	σ	1.97824	C13 - C14	σ^*	002306	3.49	1.28	0.060
			C10 - C9	σ^*	0.03654	3.33	1.19	0.056
			C10 - C15	σ^*	0.02355	3.55	1.28	0.060
O1 LP (1)	σ	1.96418	N1 - C9	σ^*	0.01826	4.21	1.12	0.062
O1 LP (2)	π	1.69272	C6 - C5	π^*	0.47150	29.66	0.33	0.092
			N1 - C9	π^*	0.31863	37.94	0.33	0.099
N1 LP (1)	σ	1.89872	O1 - C9	σ^*	0.04164	15.18	0.62	0.087
			C6 - C5	σ^*	0.04090	4.36	0.88	0.056
O2 LP (2)	π	1.81328	S1 - C3	σ^*	0.26279	17.14	0.36	0.071
	π		S1 - C2	σ^*	0.25656	21.61	0.33	0.077

[a] $E^{(2)}$ means energy of hyper conjugative interactions.
[b] Energy difference between donor and acceptor *i* and *j* NBO orbitals.
[c] F_{ij} is the Fock matrix element between *i* and *j* NBO orbitals.

Table 5 Calculated chemical parameters of the title compound at B3LYP/6-311++G(d,p) level.

Basis Set	B3LYP/6-311G++(d,p)
E_{TOTAL} (Hartree)	-1336.8994
E_{HOMO} (eV)	-6.6415
E_{LUMO} (eV)	-2.1241
[a]ΔE_{Gap} (eV)	4.5174
I (eV)	6.6415
A (eV)	2.1241
μ (Debye)	7.5110
η (eV)	2.2587
χ (eV)	4.3828
σ (eV)	0.4427
μ_p(eV)	-4.3828
ω	9.6045

E_{TOTAL}: Total energy
E_{HOMO} and E_{LUMO}: Energy values of HOMO and LUMO
μ: Total molecular dipole moments,
[a]$\Delta E_{Gap} = (E_{LUMO} - E_{HOMO})$: gap of energy,
I: Ionization potential,
A: Electron affinity,
η: Absolute hardness, $(I-A)/2$,
χ: Electronegativity, $(I+A)/2$,
σ: Softness, $1/\eta$,
μ_p: Chemical potential, $-(I+A)/2$
ω: Electrophilicity, $\mu_p^2/2\eta$.

Table 6 The comparison of the values first hyperpolarizability (β) for similar benzoxazoles compounds

Compound	β(cm^5/esu)x10^{-30}	Basis set
5-ethylsulphonyl-2-(p-ethylphenyl)-benzoxazole (**L**)	6.9285	B3LYP/G-311++G(d,p)
5-ethylsulphonyl-2-(o-chlrorobenzly)benzoxazole[a]	2.01	B3LYP/G-311++G(d,p)
5-nitro-2-(4-nitrobenzyl) benzoxazole[b]	8.47	B3LYP/6-3G*
2-(4-bromobenzyl)-5-ethylsulphonyl-1,3-benzoxazole[c]	3.30968	B3LYP/G-311++G(d,p)
1,2-benzoxazol-3-ylmenthane sulfonamide[d]	0.5205	B3LYP/6-31G(d,p)

[a][56] Mary *et al.*, 2012.

[b][61] Bhagyasree *et al*., 2013

[c][15] Zeyrek *et al.*, 2015.

[c][62] Muthu *et al.*, 2014.

Table 7 Binding affinity of different poses of the investigated ligand (**L**) as predicted Autodock Vina.

Compound-inhibitor	Mode	Affinity (kcal/mol)	Distance from best mode RMSD l.b.	RMSD u.b.
L- (NADPH)				
	1	-8.8	0.000	0.000
	2	-8.4	1.462	1.968
	3	-8.2	2.989	8.518
	4	-8.0	31.285	32.845
	5	-7.8	31.621	33.558
	6	-7.8	1.809	2.360
	7	-7.8	3.376	8.592
	8	-7.8	34.020	35.883
	9	-7.7	31.493	33.404
L-(B-DNA)				
	1	-8.0	0.000	0.000
	2	-7.9	1.386	2.364
	3	-7.3	17.864	20.411
	4	-7.2	20.002	22.234
	5	-6.9	20.508	22.550
	6	-6.8	1.856	2.424
	7	-6.7	22.465	24.399
	8	-6.4	22.408	24.372
	9	-6.4	20.607	23.032

L: *5-ethylsulphonyl-2-(p-ethylphenyl)-benzoxazole*

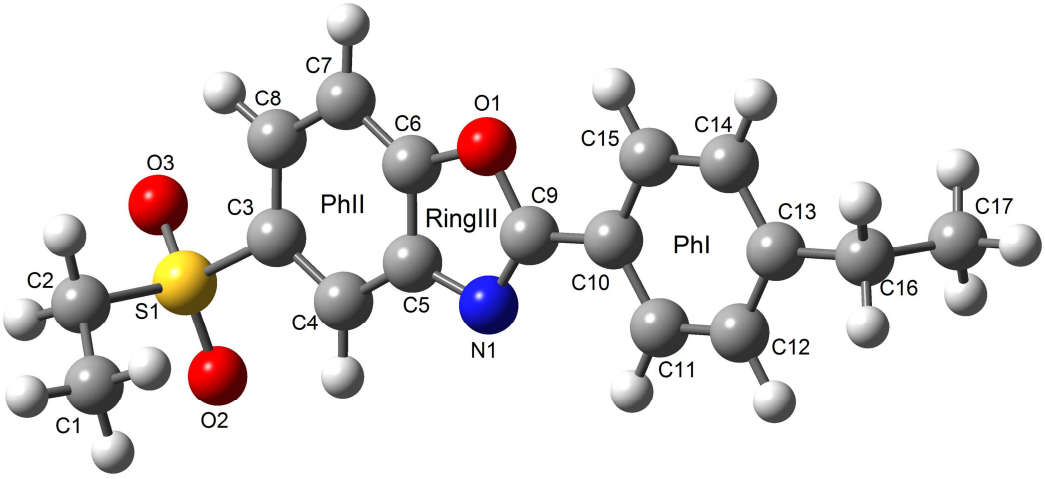

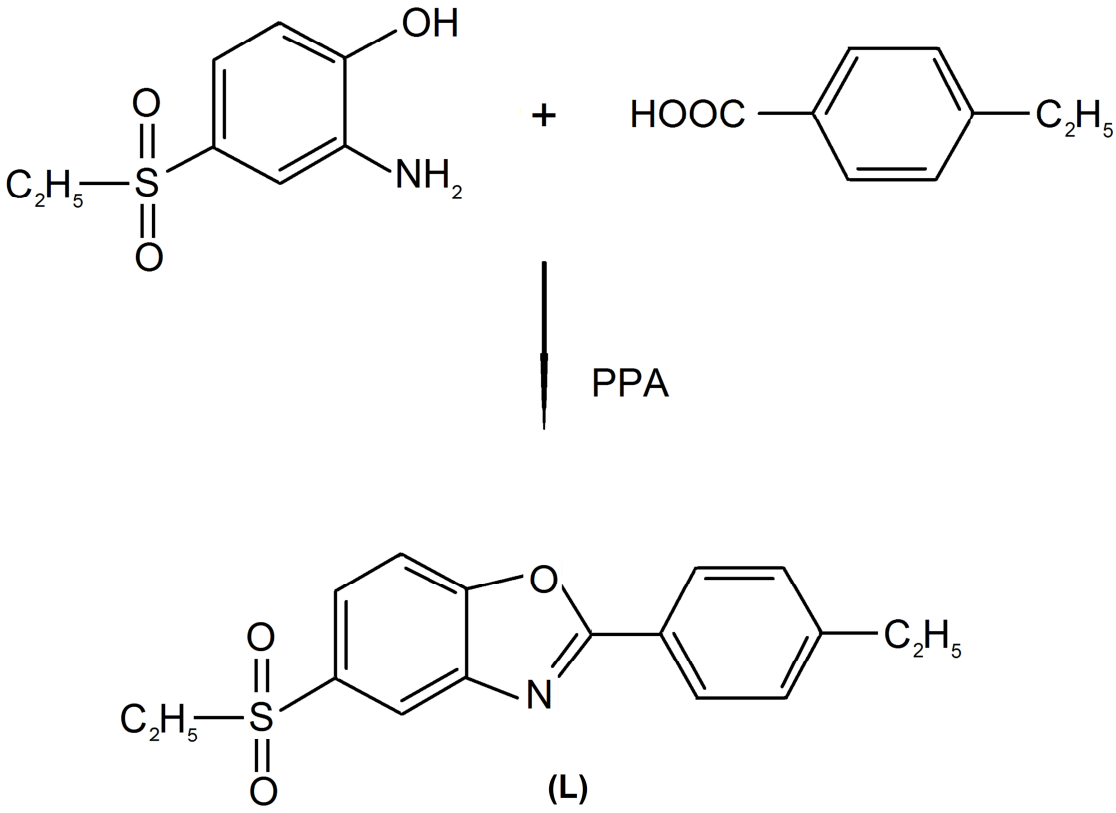

(L)

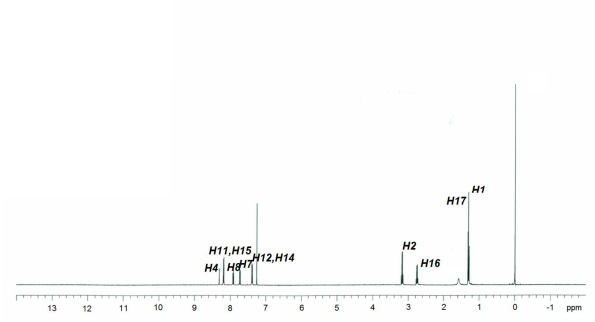
H11,H15
H4
H8
H7
H12,H14
H2
H16
H17
H1
13 12 11 10 9 8 7 6 5 4 3 2 1 0 -1 ppm

(a)

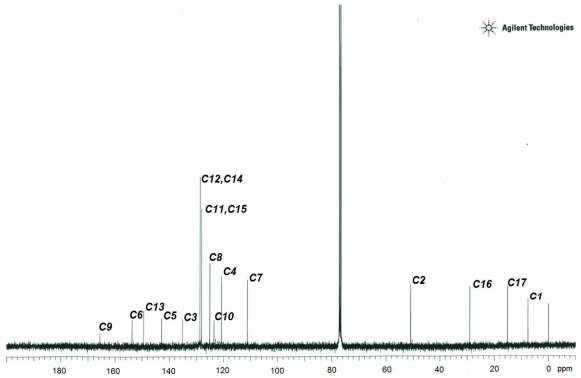
Agilent Technologies
C12,C14
C11,C15
C8
C4
C7
C2
C16
C17
C1
C9
C6
C13
C5
C3
C10
180 160 140 120 100 80 60 40 20 0 ppm

(b)

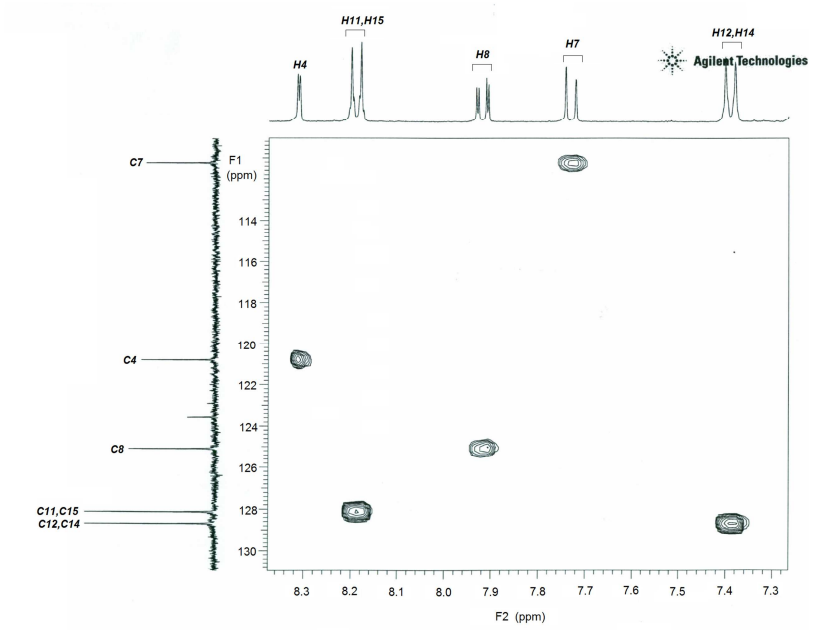
H11,H15
H4
H8
H7
H12,H14
Agilent Technologies
C7
C4
C8
C11,C15
C12,C14
F1 (ppm)
114
116
118
120
122
124
126
128
130
8.3 8.2 8.1 8.0 7.9 7.8 7.7 7.6 7.5 7.4 7.3
F2 (ppm)

(c)

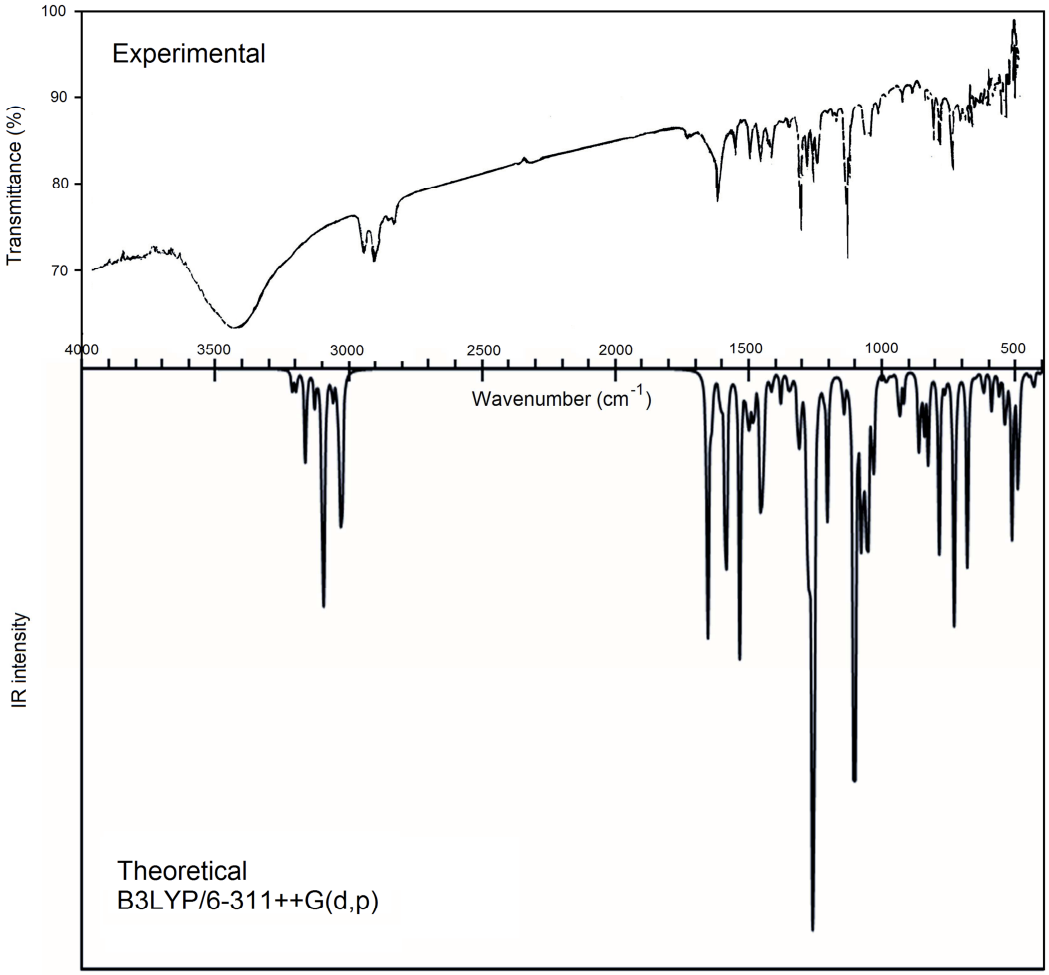
Experimental
Transmittance (%)
100
90
80
70
4000
3500
3000
2500
2000
1500
1000
500
Wavenumber (cm-1)
IR intensity
Theoretical
B3LYP/6-311++G(d,p)

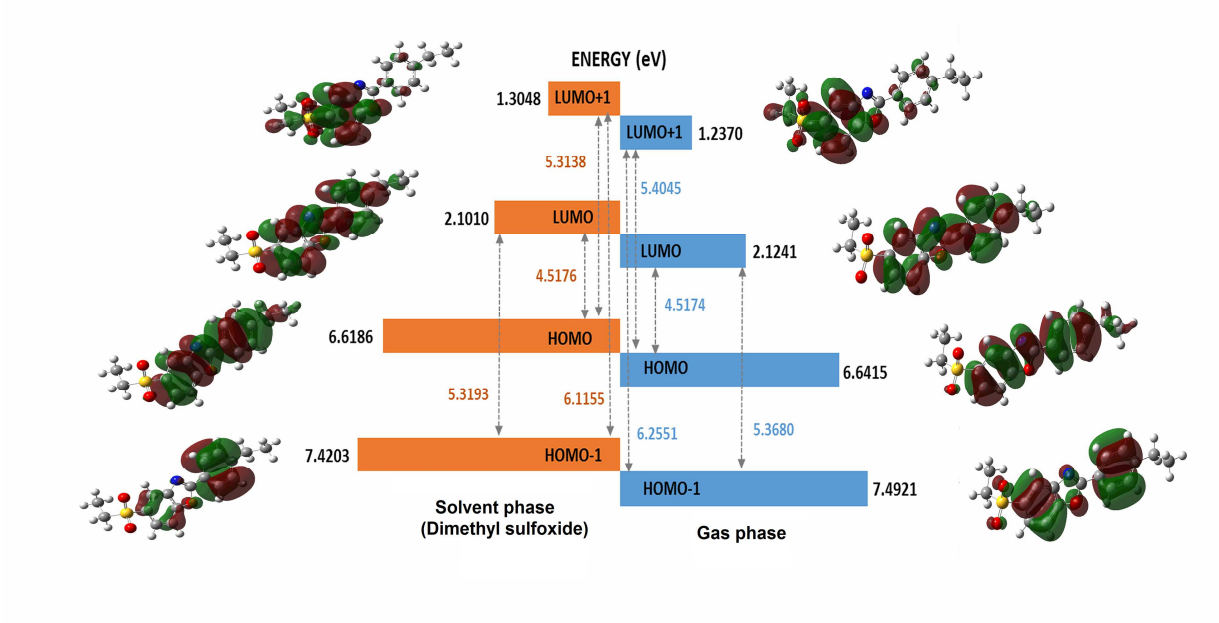

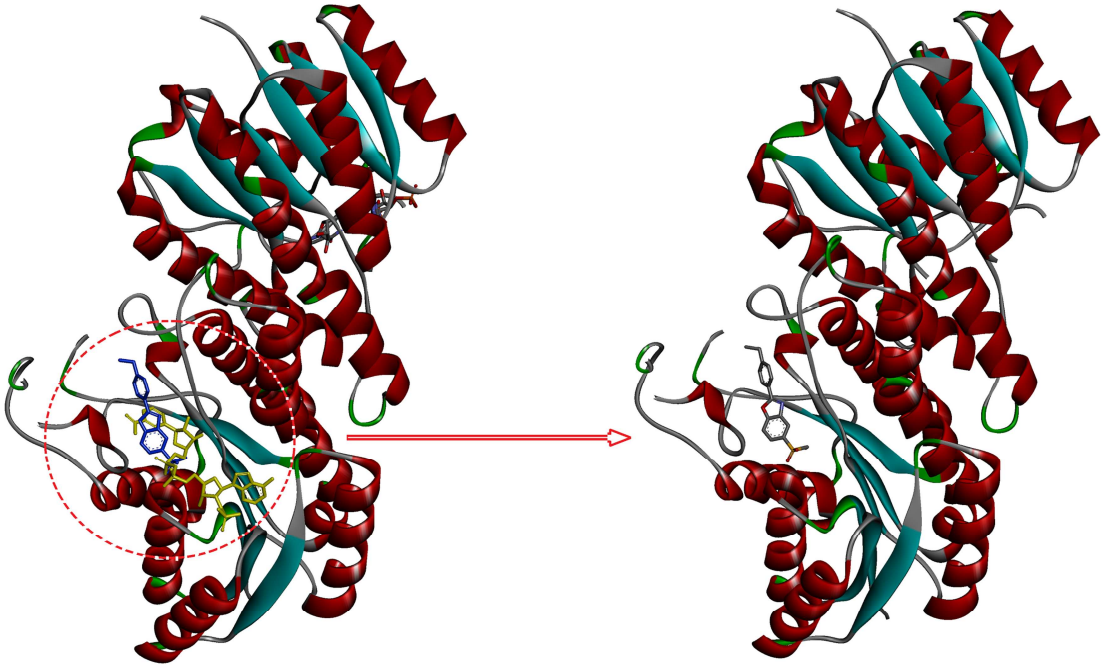

(a) (b)

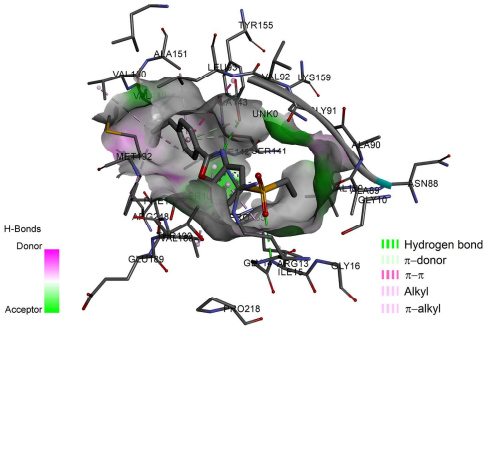

(a)

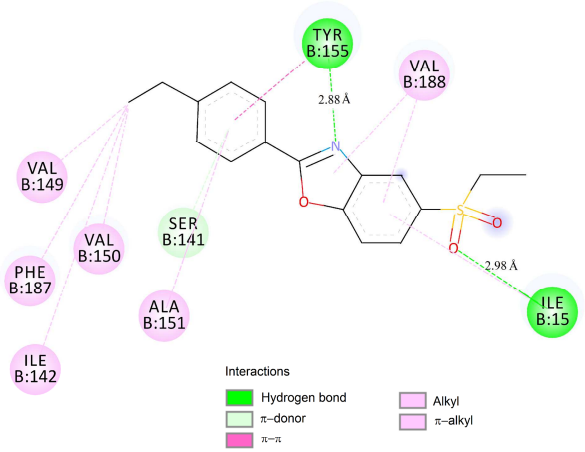

(b)

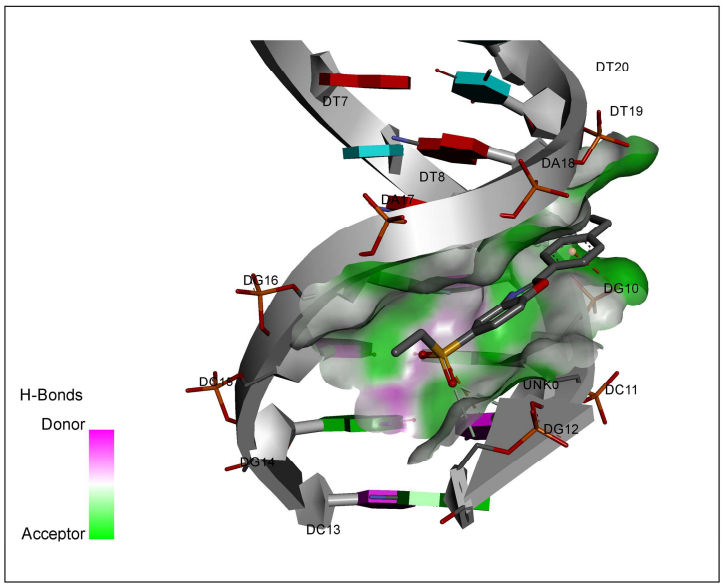

(a)

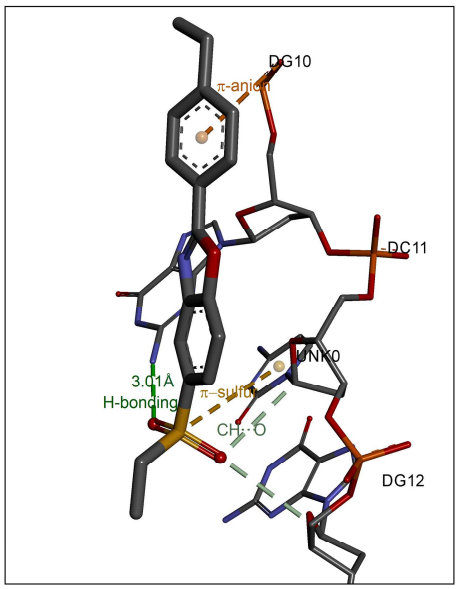

(b)

Highlights

- The 5-ethylsulphonyl-2-(p-ethylphenyl)-benzoxazole (**L**) has been synthesized.
- Density functional modelling studies of the title compound have been reported.
- The calculated vibrations show good agreement with the experimental results.
- The antibacterial activity of the title compound has been investigated.
- Molecular docking studies of **L** with an oxidoreductase enzyme and DNA have been performed.